Master's Thesis

Master's Degree in Thermal Engineering

Analysis of automotive thermal management heat exchangers

REPORT

Author: Ernest Palacios Surribas
Director: Carles Oliet Casasayas

Semester: Spring 2022

Escola Tècnica Superior
d'Enginyeria Industrial de Barcelona

Abstract

This work is focused on a specific application in the field of heat exchangers, and that is a vehicle radiator. Specifically, the project consists of the design and implementation of a code using the MATLAB environment to simulate the thermal behavior of a typical aluminum louvered fin automotive radiator. The methodology used to solve the equations is the ε-NTU and multi ε-NTU method. The working conditions and detailed geometry are defined, and it is explained the algorithm used to solve the problem, and also the specific correlations selected for the calculation of heat transfer and pressure loss, for this kind of heat exchangers.

Beyond simulation part, it is also studied the State-of-the-Art of automotive radiators, to have an idea on the recent ideas, methods and ultimate technology applied in this field. In this part it can be seen some very different technologies implemented, which all of them are focused on improving the thermal performance of vehicle radiators. Taking into account the State-of-the-art part, it is implemented one of these novel technologies to the simulation developed in the project. In this case, it is the use of a nanofluid as a coolant in the radiator, with the aim of improving the thermal behavior. Specifically, the nanofluid used in the simulation is water + Al_2O_3 nanoparticles.

The results obtained with the code developed show the heat transfer behavior of the radiator for certain mass flow rates conditions, and they are compared with other experimental results, demonstrating that the code works well enough, despite that the obtained results could be more accurate. The results for the implementation of nanofluid coolant in the simulation also show a clear improvement in the heat transfer rate.

Summary

1. Nomenclature

H: Total height [m]

D: Total depth [m]

L_{total}: Total length [m]

Ft: Fin thickness [m]

Fl: Fin length [m]

Fp: Fin pitch [m]

Fd: Fin depth [m]

Dm: External tube diameter [m]

Di: Inner tube diameter [m]

Tt: Tube thickness [m]

Tp: Tube pitch [m]

Td Tube depth [m]

Ts: Separation between tubes [m]

Ll: Louver length [m]

Lp: Louver pitch [m]

Lh: Louver height [m]

θ: Louver angle [degrees]

N_{fins}: Number of fins

S: Section [m^2]

Per: Perimeter [m]

air: Certain variable for air

liq: Certain variable for liquid or coolant

Dh: Hydraulic diameter [m]

A: Heat transfer area [m^2]

nf: non finned

f: finned

$\dot{m}$: Mass flow rate for a single tube [Kg/s]

$\dot{m}_{total}$: Total mass flow rate [Kg/s]

N: Number of control volumes

N_{tubes}: Number of tubes

L: Control volume length [m]

ε: efficiency in ε-NTU method

$\dot{Q}$: Heat transfer rate [W]

NTU: Number of transfer units

Z: Z parameter in ε-NTU method

μ: Viscosity [Pa s]

ρ: Density [Kg m^{-3}]

λ: Thermal conductivity [W m^{-1} K^{-1}]

Cp: Specific heat [J Kg^{-1} K^{-1}]

V: Velocity [m s^{-1}]

Re: Reynolds number

Pr: Prandtl number

j: Colburn coefficient

Nu: Nusselt number

α: Heat transfer coefficient [W m^{-2} K^{-1}]

f: Friction factor

τ: Shear stress [Pa]

lam: Laminar regime

$turb$: Turbulent regime

$wall$: Variable value at wall

η_f: Fin efficiency

η_0': Fin Surface efficiency

U: Overall heat transfer coefficient [W m^{-2} K^{-1}]

in: Inlet condition

out: Outlet condition

T: Temperature [K]

P: Pressure [Pa]

new: Recalculated value of a certain variable

$Next\ iter$: Next iteration value of a certain variable

δ: Convergence criteria value

α: Rectangle sides ratio

nfl: Nanofluid

bfl: Base fluid

$npart$: Nanoparticle

φ: Nanofluid volume concentration [per unit]

d: Nanoparticle size [nm]

2. Introduction

2.1. Motivation

The motivation for this project is the fact of being able to study a type of device that is very common in the world of thermal engineering, such as a heat exchanger, and more specifically a vehicle radiator, which is a very common application in real life.

The current situation of the automotive world, with the incorporation of electric vehicles and new changing technologies, means that the study of these types of radiators is also a motivation to learn about the current situation in this field and to see how they adapt to these changes.

On the other hand, the fact of being able to develop a code that simulates thermal behavior is also a motivation, given the current situation in the world of engineering and science, where programming is both a useful and basic tool.

2.2. Project objectives

The aim of this project is to understand the thermal behavior of a typical louvered fin automotive radiator, in order to be able to design better radiators. To achieve that, a code is developed to simulate the thermal behavior of a radiator of this kind. Following this main objective, it is wanted to create a versatile code that allows to correctly simulate the thermal behavior, obtaining coherent results, and allowing to modify certain parameters and variables of the simulation in an easy way. Another objective is to correctly apply the methodology used to solve the problem, in this case the simple and multiple ε-NTU, demonstrating knowledge in the theory of heat exchangers. It is also wanted to know the current technological trends in the field of vehicle radiators, by researching on the current State-of-the-art in this field, and on this basis, try to implement some kind of enhancement, by using the developed code. It would be interesting to confirm an enhancement of the heat transfer performance by analyzing the obtained results.

2.3. State of the art on Automotive radiators

This section of the project aims to inform about the state of the art in car radiators. The state of the art in any engineering field has a huge importance, as it establishes the base to know where the next investigations should be directed to. It gives a general idea on how a concrete engineering topic has evolved in time and what are the actual efforts that are being done in order to continue its evolution.

In this project case, the state of the art of car radiators is absolutely useful to give us an idea about how car radiators technology is changing. It has to be seen a lot of different aspects such as if there are any trends in vehicles production that affect the radiators characteristics, or if there is any significative change in car radiators geometry, if new materials are being proposed for production, if new coolants are being considered, or what are the parameters that are trying to be improved (efficiency, heat transfer rate, friction losses, etc.), between other possible issues.

In the next subsections some actual techniques and studies are being explained in order to have a wide idea about the state of the art of automotive radiators.

2.3.1. Proposal of an electric vehicle finless heat exchanger

The electric vehicle (EV) is an emerging market that is increasing sales year by year [2], and it is positioning as a solid alternative to the internal combustion engine (ICE) cars in the transition to a net zero scenario. This transition from ICE to EV needs to be done in the very next years, due to the rush to replace ICE vehicles in transport world, as the consequences related with climate change are already present in our world and society.

Regarding this situation, Samiolo and Verdin (2022) [1] proposed a solution for radiators in electric vehicles. Their idea is to design a radiator taking into account that the transition to EV has to be done quickly. Therefore, the aim is to take advantage from the already existing processes of production of the parts and devices of the current ICE vehicles, in order to not have to change the entire line of production. In this way, the economic affection to the cars manufacturers would be less important. In terms of the radiator, it is wanted to keep a similar layout and not modify completely the front part of the vehicle. It is important to know that the change from ICE to EV vehicles can bring some advantages such as the less need to dissipate heat, as the combustion engine is removed. On this context, the prioritized characteristics for the radiator are cost, aerodynamic efficiency or lightness between others, but not the thermal characteristics, as the thermal performance of the EV is less demanding.

The proposal of Samiolo and Verdin (2022) [1] is a new design with a lower cost by reducing the complexity of the conventional car radiators, but keeping some good characteristics already present. The new idea consists of substituting the fins of the radiators by a dimpled pattern of surfaces like the ones in Figure 1. Dimpled surfaces have been used in different

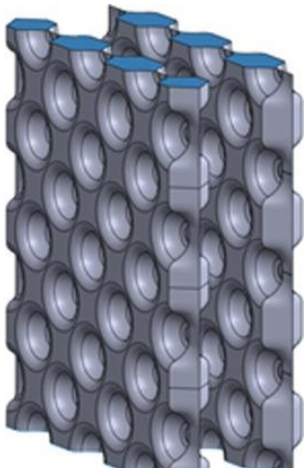

Figure 1. Dimpled surfaces. [1]

technical applications and devices but usually they have not been considered as a heat dissipation element. The role of the dimples is to create vortices in between the surfaces, and by this way creating a recirculation fluid movement that works as a source of cold air. This design would reduce production costs and would also bring a lower weight / volume ratio.

An initial dynamic and thermal study were done with CFD analysis and by using RANS models, and after that the authors could reach some conclusions. It showed that a reduction of 5% of drag force, and a sufficient heat dissipation could be achieved, despite the fact that the new heat exchanger is not as good as the previous ones in thermal performance, but it is cheaper and lighter. The authors also confirm that further research would be required through experimental and also CFD studies. Nevertheless, this proposal gives a clear point of view of a possible evolution of ICE radiators to adapt to EV radiators, taking into account that production costs have to be reduced and it is wanted to affect the minimum possible to the actual car radiators production processes in order to make the transition from ICE to EV as quick as possible.

2.3.2. Nanocoating in heat transfer enhancement

This topic is related with surface engineering. Surface engineering aims to modify the surface properties of a specific component in order to achieve some functional desires. Some uses of surface engineering are friction reduction, improve resistance to corrosion, or change the

mechanical properties of a component, between others. Another functionality of surface engineering is to increase heat transfer, for example, by nanocoating of the tubes of heat exchangers.

Nano-coatings are very thin layers of nanoparticles or chemicals structures that are built upon surfaces [3], they could be described as any substance that has one or more components sized on the nanometer scale and the main components is called the matrix [9]. Nano-coatings are of interest as they could allow an enhancement in heat transfer performance of the surface. For this reason, this kind of technology has been investigated and some literature, experiments and studies have been carried out, as it could be a good solution in some applications related with heat transfer phenomena, such as heat exchangers, or more concretely, car radiators. The research on optimization of radiators is absolutely present nowadays, as car industry has an important role in economic world, so this type of possible better performance solutions are always taken into account, and it has to be seen if nano-coatings could be a good implementation in car radiators.

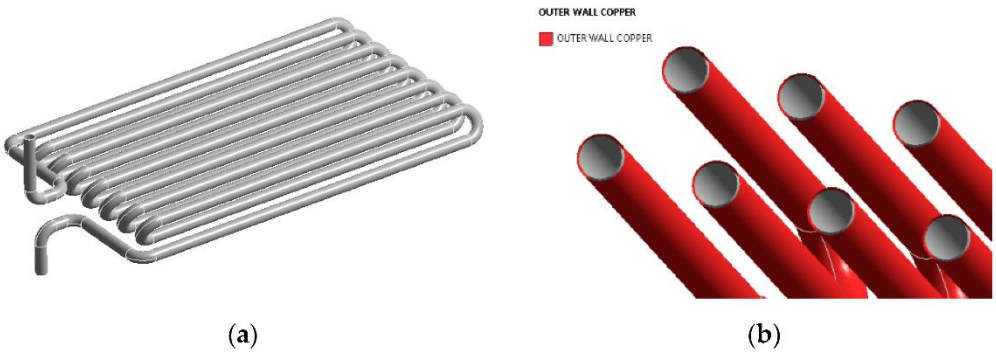

Figure 2. Nanocoated tube in Pungaiah and Kailasanathan simulation. [4]

Some experiments have been done by now: Pungaiah and Kailasanathan (2020) [4] made a simulation using CFD and Taguchi method in a circular tube with nano-coating on its external surface. The tube was like the one in Figure 2, and the experiment consisted on the water going through the tube at three different mass flow rates of 0,15, 0,30, 0,45 L/min, with three different possible inlet temperatures of 323 K, 343 K, 363 K, and three different thickness for the cooper nanocoating of 50, 80 and 100 μm, while considering the air from the exterior at 25ºC. Pungaiah and Kailasanathan (2020) concluded that the effect of the coating improves the heat transfer rate for all the different conditions of flow rate and inlet temperature, but the thickness of 100 μm is the one that provides better heat transfer performance. It was concluded that the thickness plays a significant role in the results.

In another study, Pungaiya and Kailasanathan (2018) [5] researched about the use of thermal spray technology, which consists of fusing material in a spray gun and atomizing the drops of this material onto a surface, where the fused material becomes a thin coating. The

authors concluded that in general there's a heat transfer enhancement when using thermal spray technique and they also report that thermal spray technique is one of the best for modifying the thermal conductivity of a surface, as an advantage is the wide range of materials that can be used as substrate and coating compounds. Focusing on the case of automobile radiators, the authors expect an increment in heat transfer coefficient of the surface and a considerable enhancement also in the overall heat transfer coefficient of the radiator.

Sujith Kumar, Suresh and Rajiv (2012) [6] made an experimental study of heat transfer and mechanical characteristics of a Carbon Nanotube (CNT) coating on a steel surface of a rectangular macro-channel, where the working fluid was water. CNT coating techniques are usually implemented by Chemical Vapour Deposition (CVD). The experiment was performed under both laminar and turbulent flow conditions, and with and without the coating. The results showed clearly a greater heat transfer rate for the coated surface than for the uncoated, and the authors attribute this improvement to the increase of roughness of the surface that caused local turbulence. They also emphasize that the better thermal performance was not followed by a significant increase of the pressure drop. It could also be observed that the enhancement in Nusselt number was more significant in the laminar region than the turbulent region.

Another study was performed by Rajput and Kulkarni (2014) [7], it was about the effect of perforating fins and using CNT coating at the same time, in order to increase heat transfer. They researched among the existing literature, and found out that CNT coating can be useful as it seems clear that enhances the heat transfer rate.

Jadar, Shahishekar and Manohara (2016) [8] implemented nanotechnology in a conventional car radiator. They focused on multi-wall carbon nanotubes (MWCNT) as the new material to introduce in the automotive heat exchanger with the purpose of improving the heat transfer performance. Car radiators fins are usually made of aluminium, so in their study, they tried to apply the composite material Al-MWCNT (Aluminium – Multi-wall carbon nanotubes) for the fins. The experiment was performed with water as the coolant fluid, and for different mass flows from 0.5 L/min to 3 L/min. The results showed that an average enhancement of 12,26% in heat transfer coefficient was achieved with the new fin material. A reduction in weight was also an improvement due to the use of Al-MWCNT fins.

To sum up, it seems clear that nano coatings and nanotechnology can have a significant impact in car radiators performance, as there are different studies that prove thermal enhancement when using this kind of nanotechnologies. Nevertheless, it's hard to find a considerable number of experiments applied directly on car radiators, to find more reliable results and conclusions, so it's probably one engineering field to be investigated more deeply.

2.3.3. Polymeric car radiators

Another approach in the field of car radiators concerns polymeric materials. Usually, radiators and in a more general way, heat exchangers, are made of metallic materials due to its favorable thermal conductivity. Nevertheless, there have been some investigations and ongoing works about using polymers in heat exchangers devices, as although it is known that polymers have a worse thermal conductivity compared to metallic materials, they have some advantages that could compensate it. In general, plastics have some better characteristics than metals such as low weight, chemical stability, resistance to corrosion, relatively low production cost, recyclability and low fouling [11] [12] [13] [15], which can lead to having a possibility in the heat exchangers world. It is important to consider the fact that the temperatures of the working fluid in car radiators can be high, and it could alter the properties of polymeric materials, but as Zaheed and Jachuck (2004) [13] stated, a polymer can serve as an alternative to metal materials while its glass transition temperature is not reached by the working fluids in the application.

Despite that the fabrication of polymer heat exchangers has not been widespread in process industry (Zaheed and Jachuck, 2004) [13], some polymeric heat exchangers (and more concretely vehicle radiators) designs have been tested and studied, with the aim of exploiting the potential that polymers can have. For example, Jacobi and Park (2008) [10] experimented with a polymer tube-bundle heat exchanger for liquid-to-gas applications. Their idea was to compare a polymeric heat exchanger made of high temperature nylon and cross-linked polyethylene with a typical louvered fin-and-tube heat exchanger made of aluminum and cooper. Taking into account the thermal and mechanical limits of the polymers, they calculated a minimum tube thickness for a given tube diameter, and could propose the design of the polymeric heat exchanger, considering that thermal conductivity is much lower, and so, a higher heat transfer area for the polymeric heat exchanger would be required.

The two designs were like the ones in Figure 3 and Figure 4.

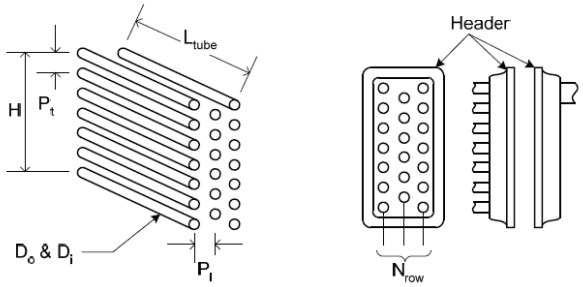

Figure 3. Polymeric heat exchanger scheme (Park and Jacobi, 2004). [10]

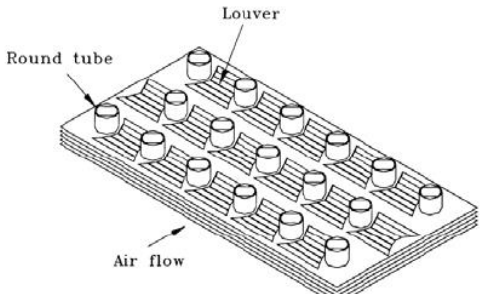

Figure 4. Louvered fin-and-tube aluminium heat exchanger (Park and Jacobi, 2008). [10]

They run a simulation using epsilon-NTU method and with water and air as working fluids, obtaining some interesting results. They could conclude that the lower thermal conductivity of polymers was overcome by using a large number of small and thin tubes, so they stated that polymeric heat exchangers were a possible alternative solution. However, they could see that the tube wall resistance could be significant if the tube is not too thin. They could verify that the most important factors to have an optimal thermal performance were small tube diameters, small tube pitches, and low fluids flow rates.

Another experiment was carried out by Krásný, Astrouski, and Raudenský (2016) [11], preparing a prototype made of polypropylene with a thermal conductivity of 0,18 W/m^2K. Their car radiator prototype consisted on 14 layers of 140 fibers connected between them, where the coolant was going through those hollow fibers. It looked like the one in Figure 5.

Figure 5. Hollow fiber automotive radiator prototype by Krásný et al. [11].

The experiment was carried out for three different inlet temperatures of 60ºC, 75ºC and 90ºC for the coolant, which was a 50%/50% water-glycol solution. Air speed varied from 2 to 10 m/s by using a fan. The experiment was realized by two slightly different prototypes, one with 0,6 mm diameter fibers, and another one with 0,8 mm diameter fibers.

After conducting the experiments, Krásný et al confirmed that the thermal performance of the

prototype radiator was comparable to aluminum radiators, overcoming the low thermal conductivity of polypropylene. They obtained an overall heat transfer coefficient up to 355 W/m^2K, and also could see that the heat transfer coefficient of the air side increased when the outer diameter of the fibers decreased. The radiator made of 0,8 mm diameter fibers had approximately a 20% higher pressure drop than the 0,6 mm diameter fiber radiator. Another interesting conclusion was that comparing the experimental results with theoretical predictions, it could be seen that Grimson equation can be used for outer heat transfer coefficient calculations.

Another study was done by Kroulíková, Kudelová, Bartuli, Vancura and Astrouski (2021) [15], which compared the thermal performance between a commercial aluminum car radiator of a Skoda Octavia with a polymeric car radiator design proposed by the authors. The aim of the study was to see the strength and weaknesses of using polymeric materials in car radiators. A remarkable characteristic that the authors present about polymeric heat exchangers is that fouling is four times slower compared with metallic louvered fins heat exchangers of similar size. For the design of the polymeric hollow fiber radiator the authors highlight the importance of the fibers distribution in order to not have performance loss due to flow dead zones and bypasses. The polymeric hollow fiber radiator consisted of 34 layers of 360 fibers each layer, with a fiber length of 480 mm, outer diameter of 0,8 mm and inner diameter of 0,64 mm, and the material was polyamide 612.

The experiment consisted in using 50%/50% ethylene-glycol/water mix as the coolant, with a coolant inlet temperature of 90ºC and air inlet temperature of 30ºC. The air velocities went from 1 to 4 m/s for the polymeric radiator, and from 2 to 6 for the metallic one, while the liquid flow rate went from 15 to 60 L/min for the polymeric radiator, and from 30 to 90 for the metallic one. The results showed that when the air velocity was between 2 m/s and 4 m/s the heat transfer rate was between 25% and 30% better for the polymeric radiator than for the typical one (for a 60 L/min liquid flow rate). The liquid pressure drop seemed similar for both types of radiators, although the authors conclude that for a higher liquid flow rate, the polymeric radiator would have less pressure drop, due to the mostly laminar regime of the liquid going through the fibers. They concluded that the maximum heat transfer rate was 30% better for the polymeric radiator, and with a 30% less of weight. Both radiators had similar coolant pressure drops for these working conditions, and the air pressure loss was much higher for the polymeric radiator. In general, the authors see polymeric hollow fiber radiators a competitive alternative for typical metallic radiators.

After regarding the present literature about polymeric heat exchangers some conclusions can be extracted. Polymeric hollow fiber heat exchangers are still not widespread in automotive industry and also there is not a huge quantity of data related with this type of radiators or heat exchangers, as Raudensky et al affirmed [14]. Nevertheless, there are experiments that have been carried out, and although all these experiments have some

different conclusions, they agree in some basic questions. For all of them seems clear that the low thermal conductivity of polymers can be overcome as the heat transfer surface can be higher than it is for the typical metallic radiators, achieving in this way, similar heat transfer rates and high global heat transfer coefficient. In terms of pressure drop, some studies such as Kroulíková et al [15] state that coolant pressure loss is similar to the metallic radiators, so it doesn't seem a special drawback, although having more experimental data would be interesting to confirm it. Another important point to consider when studying the polymeric radiators is to ensure that the working conditions temperature will not imply a degradation of material properties (Zaheed and Jachuck, 2004) [13], which could lead to a not good working of the device, thus, a careful material selection for is basic for its thermal performance (T'Joen, Park, Wang, Sommers, Han and Jacobi, 2009) [12].

All these studied thermal performances of polymeric radiators combined with the advantages of having a good resistance to fouling and corrosion, chemical stability, a lower weight per unit of volume, and a lower fabrication cost, present this type of radiators as a solid alternative solution in automotive industry, if further investigation and work is undertaken.

2.3.4. Nanofluid coolants

With the aim of increasing and improving the heat transfer phenomena in vehicle radiators, another field of research is the use of nanofluids as coolants in these devices. Nanofluids are a kind of fluid which contain low concentrations of small nano-sized particles (approximately between 1 and 100 nanometers) in a base fluid. The nano-particles are homogenously distributed in the base fluid and permanently in solid phase. The reason for using nanofluids as coolants is that the typical used fluids have a relatively low thermal conductivity compared to solid materials, which limits the heat transfer in a heat exchanger. It has been proven that nanofluids have in general a higher thermal conductivity than the base fluid without the addition of nano-particles [16], and that is seen for investigators as a point with huge potential for improving radiators and its thermal performance.

This field of research has a rather wide and diverse literature and studies, therefore, based on that, it is wanted to see how the studies of nanofluids in car radiators are focused and see if any clear conclusions can be drawn. Furthermore, beyond the study at the level of impact on heat transfer phenomena, it is important to see if the use of nanofluids is considered economically viable for large-scale implementation in normal vehicles. With this situation, some studies that have been carried out so far, and their main conclusions, are presented below.

Delavari and Hashemabadi (2014) [17] conducted an CFD simulation and also experimental study for a nanofluid passing through a flat tube. The nanoparticle they experimented with was Al_2O_3, and the concentration varied from 0,1% to 1% in volume. The base fluid was in one case water, and in the second case pure ethylene glycol. The experiments were carried out for different inlet temperature values varying from 35ºC to 60ºC. Analyzing their results, it was observed that when the concentration of nanoparticles increased, the Nusselt number and the heat transfer coefficient did so. It was also observed that the friction factor was higher when the concentration of nanoparticles in the base fluid increased, however, the authors point out that for a given heat transfer rate, the coolant flow rate would be less when using nanofluids, and that would imply less pumping power required.

Tijani and Sudirman (2018) [18] studied the thermo-physical properties and heat transfer behavior of two different nanofluids in a car radiator, by using CFD. One nanofluid was Al_2O_3, while the other one was CuO nanofluid, and in both cases the base fluid was a 50%/50% mix of water and ethylene glycol. The concentration values of nanoparticles were 0,05%, 0,15% and 0,3%, and the mass flow rate was kept constant. The results showed that the addition of nanoparticles to the base fluid improved the thermal conductivity, which was 0,415W/mK for the base fluid and increased to 1,287 and 1,241 for Al_2O_3 and CuO nanofluids respectively, when the concentration was the highest, 0,3% in volume. The heat transfer coefficient and Nusselt number also increased with the addition of nanoparticles. Nusselt number was 164,29 for the base fluid and turned to 173,19 and 208,71 for Al_2O_3 and CuO nanofluids respectively, with a 0,3% concentration of nanoparticles. They could affirm that CuO nanofluid showed a better heat transfer performance than Al_2O_3.

Similar to the work commented before, Vajjha, Das and Namburu (2010) [19] also worked with Al_2O_3 and CuO nanofluids to compare their thermal behavior. In their numeric study, the flow regime was always laminar, with Reynolds number taking values of 100, 200, 500, 1000, 1500 and 2000, and the concentrations in volume of nanoparticles varied from 0% to 10% for the Al_2O_3 and from 0% to 6% for the CuO. The base fluid was 60% ethylene glycol, 40% water. The results obtained in their simulation for a flat tube were that the heat transfer coefficient and friction factor increased when increasing the concentration of nanoparticles. It was found that for 10% concentration of Al_2O_3 when Reynolds had a value of 2000, the heat transfer coefficient was 94% higher than the value of the base fluid at the same conditions, showing an important improvement. A similar improvement was found for the CuO nanofluid, which maximum improvement of the heat transfer coefficient was 89% higher than the base fluid. Nevertheless, the authors emphasize that the Reynolds number influence in heat transfer coefficient enhancement is stronger than the concentration of nanoparticles. Another important conclusion is that the augmentation of friction factor, as for a 0,39 m/s inlet velocity and 6% CuO nanofluid the friction factor was 2,75 times greater than the friction factor of the base fluid at the same conditions.

Following with the studies of Al_2O_3 and CuO nanofluids, Epandi, Salami Tijani, Abdulrahman, Kubenthiran and Muritala (2022) [20] made a CFD simulation to investigate the heat transfer characteristics of Al_2O_3 and CuO nanofluids in a flat tube of a car radiator. The base fluid was 20% ethylene glycol and 80% water, and the volumetric concentrations of nanoparticles varied from 0,05% to 0,3%. Similar to the results that Tijani and Sudirman (2018) [18] found, Aisyah et al found that the thermal conductivity augmented from 0,415 W/Mk to 0,9285 W/mK and 0,9042 W/mK for Al_2O_3 and CuO nanofluids, respectively, when the concentration value was 0,3%. The Nusselt number also augmented from 94,51 of the base fluid to 101,36 for Al_2O_3 and 130,46 for the CuO nanofluid, showing an improvement, which was even greater when the concentration of nanoparticles increased. In fact, they registered a 10% increase in the heat transfer coefficient when the concentration was 0,3% in comparation to when it was 0,05%. In general, they reached similar conclusions to Tijani and Sudirman (2018), expressing that CuO nanofluid showed a better heat transfer performance than Al_2O_3 nanofluid.

Other particles have been also studied for these applications. For example, M. Hussein, Bakar, Kadirgama and Sharma (2014) [20] experimented with a car radiator with flat cooper tubes. In this study, TiO_2 and SiO_2 nanofluids were used, with water as base fluid. The Reynolds number for the coolant ranged between 250 and 1750, and the concentration of nanoparticles ranged between 1% and 2,5%. The authors reached an interesting conclusion that differs from the ones found in other articles and works, as according to their results, the friction factor augmentation when increasing the nanoparticle concentration was insignificant, as it varied less than 3%. Nevertheless, the results showed an improvement of the heat transfer performance when using nanofluids compared to the base fluid, as the Nusselt number increased with the concentration of nanoparticles. When the concentration had a maximum value of 2,5%, the Nusselt number was nearly the double of the pure base fluid, reaching maximum values of 16,4 and 17,85 for TiO_2 and SiO_2, respectively, in laminar flow. The authors conclude that Nusselt number is always a bit higher for SiO2 nanofluid. In terms of heat transfer rate, it could be seen that it increases with flow rate and with nanoparticles concentration, achieving a higher maximum heat transfer rate for SiO_2 (74W) than for TiO_2 nanofluid (63W). The enhancement in heat transfer rate respect to the pure base fluid is 20% and 32% for TiO_2 and SiO_2, respectively. The authors justify this better heat transfer rate for SiO_2 nanofluid due to a higher mean velocity of the SiO_2 nanoparticles, as they are less dense than TiO_2 ones.

The same authors, Hussein et al (2014) [22] did also an experimental work using TiO_2 and SiO_2 nanofluids flowing through a car radiator. They experimented under laminar flow conditions, varying the coolant flow from 2 liters per minute to 8 liters per minute, and also varying the inlet temperature between 60ºC and 80ºC. In this experiment the volume concentration of nanoparticles went from 1% to 2,5% in 0,5% intervals, and the base fluid

was pure water. In this study they could conclude a maximum Nusselt number improvement of 11% and 22,5% for TiO_2 and SiO_2, respectively, compared with the pure base fluid, and highlight the Nusselt number strong dependence with coolant flow, and also a more slightly dependence with nanoparticle concentration and inlet temperature. They also state that SiO_2 nanofluid has in general a better thermal performance than TiO_2 nanofluid. The authors did not comment the friction factor behavior although it is an important variable to take into account in these heat exchangers.

Another experimental work was carried out by Ruey, Eqhwan, Yapp, Maksudur, Khan and Anuar (2022) [23]. They experimented with SiO_2 nanofluid through a car radiator, with SiO_2 nanoparticles from 0% to 1% concentrations in a base fluid of ethylene glycol water mix. Basically, the authors highlight an improvement of the heat transfer coefficient proportional to the volume concentration of the nanofluid, and also an enhancement in heat transfer rate compared to the pure base fluid. In this study, the authors strongly believe in the use of nanofluids as a good option to be implemented in car radiators industry, and also in a more general way, in heat transfer applications. They underline the fact that the size of the vehicle's radiators could be reduced with the use of nanofluids and that would provide benefit to different aspects of the car.

Ramadhan, Azmi, Mamat, Diniardi and Hendrawati (2022) [24] investigated experimentally with a three-hybrid nanofluid in a car radiator. The nanoparticles used were Al_2O_3, TiO_2 and SiO_2, and the base fluid was a mix of water and ethylene glycol at 60% and 40%, respectively. The experiment was run changing the concentration of nanofluid from 0,05% to 0,3% with four different values, and also varying the coolant flow rate from 2 to 12 liters per minute. The inlet temperature of the coolant and the air velocity were kept constant during the experimentation, with values of 70ºC and 4 m/s, respectively. They observed the maximum heat transfer rate enhancement when the concentration was the highest of 0,3%, and the improvement was 39,7%. The overall heat transfer coefficient is also higher with the 0,3% concentration. In the same line as other studies, it was also concluded that the pressure drop increased when the concentration of nanofluid did so.

Different nanoparticles than those presented so far have also been used in nanofluid experiments on car radiators. It is the case of the study carried out by Prasanna, Banapurmath, D'Souza, Sajjan, Ayachit, Yunus, Badruddin and Kamangar (2022) [25], who used graphene oxide (GO) nanofluid. They experimented with different proportions of ethylene glycol and water as base fluid (50/50, 60/40, 30/70, 20/80) and with a volume concentration of the nanofluid of 0,1%. Coolant flow rate ranged between 180 and 420 liters per hour and the inlet temperature was kept constant with a value of 90ºC. They stated that the base fluid that showed a better thermal performance was the 60% ethylene glycol and 40% water, obtaining a 42,77% of enhancement in heat transfer rate when the coolant flow rate is 300 liters per hour, and a maximum heat transfer coefficient enhancement of 69,7%

when the coolant flow was 420 liters per hour. The authors also point out the necessity of future works on the geometry of the nanoparticles and the behavior of the nanofluids at higher temperatures.

Another experiment was carried out by Tafakhori, Kalantari, Biparva and Peyghambarzadeh (2021) [26]. The nanoparticles they experimented with were Fe_3O_4 28 nm sized, and the base fluid was water. In their experiment, the concentration of the nanofluid ranged between 0% and 0,9%, and three different inlet temperatures for the coolant were selected, which were 72ºC, 80ºC and 88ºC. The air flow rate varied on 4 different values depending on the fan power, while the coolant flow rate was kept constant. Despite that, the Reynolds number varied in a small range between 30 and 100 due to the change of nanoparticles concentration in the nanofluid, so the flow regime was always laminar during all the experiment. Tafakhori et al concluded that the maximum heat transfer rate was when the concentration was 0,1%, with an enhancement of 21% in comparison to the base fluid. This experiment brought some interesting conclusions, which differ from those obtained in other similar studies. It was seen that for a higher than 0,1% of nanoparticles concentration there was a heat transfer deterioration, so the optimum was found in 0,1% concentration. Nevertheless, the maximum thermal conductivity of the nanofluid was found with the maximum concentration of 0,9%. This suggested that thermal conductivity is not the only responsible of enhancing the heat transfer performance. The authors also highlight the significant increase of the pressure drop when increasing the nanoparticles concentration, due to the augmentation of nanofluid viscosity. This conclusion on pressure drop contrasts with the one reached by Hussein et al [21] where friction factor raise was found not significant at all.

After the research on all these studies about the possible implementation of nanofluids in car radiator applications, some conclusions can be drawn. Firstly, there's considerable amount of literature related with this topic, and all studies do not work in exactly the same conditions, so it's not easy to strongly affirm which is the nanofluid impact in the thermal behavior of a car radiator. However, in general, great part of the articles attribute a better heat transfer performance to the use of nanofluids in car radiators, so at least it is for sure a field with great potential for the future. It also seems clear that the addition of nanoparticles to a base fluid improves the thermal conductivity, as it is stated by Pordanjani et al (2019) [27], based on a huge range of literature and studies. Although that a major part of the studies previously commented coincide that the heat transfer performance is better when increasing the nanoparticles concentration, Pordajani et al question such behavior when the coolant flow is turbulent. It also has been seen that in general the addition of nanoparticles increases the pressure drop, although some studies have found insignificant this augmentation. It has been possible to see that there are mainly between 5 to 10 different nanoparticles that are used for this kind of applications, and all of them have their particularities, so it also difficulties a

generalized prediction of the behavior of nanofluids, as it depends on each nanoparticle. It was also seen that in some studies the maximum nanofluid concentration is near 0,3% while in other studies it reaches near 3%, implying that it is not clear at all where's the optimal range of nanofluid concentration. Thus, the enhancement of heat transfer rate or the enhancement of other variables such as heat transfer coefficient or the overall heat transfer coefficient depend a lot on the conditions of the experiments that have been carried out, making it difficult to exactly know how much better it is the use nanofluids.

There are also some interesting conclusions reached by Zhao, Li and Yang (2016) [28], who highlight that with the actual experimental data from literature there's a lack of knowledge on how the nanoparticle type, the temperature or the nanoparticle size affect the thermal conductivity and viscosity of nanofluids. Zhao et al [28] state that more comprehensive experimental analyses are needed in order to improve the modelling of nanofluids thermal conductivity and viscosity. They also highlight the discrepancies that different studies present on the enhancement obtained, and points out that some contradictory results on the nanoparticles concentrations make it difficult to understand more exactly the behavior of nanofluids.

Another conclusion reached after reviewing the actual literature on this topic is that not much analyses has been done on how nanofluids could became a well-established option in car radiators industry. In fact, Zhao et al [28] also indicate that the implementation of nanofluids in car radiators in a large-scale production could become limited if their cost is too high, as production cost has a very important weight in vehicles industry. Thus, this economic issue could become a limitation for nanofluids field.

3. Radiator simulation

3.1. Model

3.1.1. Methodology

The methodology implemented to simulate the car radiator is the multi ε-NTU method, and it is applied for only one of the flat tubes of the radiator. In the following points it is explained what this method consists of, and how it is applied in this study case. It is also explained why it is only applied on one tube of the heat exchanger. The calculations of the different variables needed to solve the problem are explained in the next part.

3.1.1.1. ε-NTU and multi ε-NTU method

The ε-NTU method is typically used in heat exchangers, and consists on expressing the heat transfer rate as a hypothetical maximum heat transfer rate multiplied by effectiveness (ε), as it can be seen in the following expression:

$$\varepsilon = \frac{\dot{Q}}{\dot{Q}_{max}}$$

(1)

The maximum heat transfer rate $\dot{Q}_{max}$ is understood as the maximum heat that would be transferred by an ideal heat exchanger that works at the same input conditions than the real one, with counter flow and infinite heat transfer area. Thus:

$$\dot{Q}_{max} = (\dot{m}Cp)_{min}(T_{1i} - T_{2i})$$

(2)

Implementing mathematical formulations in the heat exchanger, consisting on applying energy balances and analytically integrating along the whole heat exchanger, it is obtained the efficiency ε in function of two new parameters NTU and Z, defined as:

$$NTU = \frac{U_0 A_0}{C_{min}}$$

(3)

$$Z = \frac{C_{min}}{C_{max}}$$

(4)

The expression of ε in function of NTU and Z depends on the heat exchanger type and flow configuration, and in this study case, a cross-flow heat exchanger with both fluids unmixed, the expression of ε is:

$$\varepsilon = 1 - \exp\left(\frac{(\exp(-NTU^{0,78} * Z) - 1) * NTU^{0,22}}{Z}\right)$$

(5)

The ε-NTU is an analytical method, and in order obtain the analytical solution it is needed to take the following assumptions:

- Steady state flow.
- Constant thermo-physical properties for the whole domain.
- Constant surface heat transfer coefficients.
- One dimensional analysis (T(x)).
- There are not axial heat transfer phenomena.
- Adiabatic exterior wall (thermally isolated heat exchanger).

In order to be able to simulate the thermal performance of the heat exchanger, it has been decided to analyze just one of the twelve tubes that the radiator has, and half of the upper fins and half of the lower fins. In this way, the adiabatic exterior wall assumption is accomplished, as if the contiguous tubes are at similar temperature (usual situation), then just at the middle length of the fins $\frac{dT}{dx} = 0$, which acts as an adiabatic isolation of the tube. The only tubes that are not thermally isolated are the extreme tubes, as the heat exchange with the exterior is not controlled. Apart from this, there are no other important effects that differentiate the tubes from each other, which consolidates that by symmetry the study is simplified to a single tube.

As said before, with this condition, the study case is reduced to one tube and half of the upper fins and half of the lower fins. In Figure 6, it can be seen a scheme of the volume of the study case shaded in red.

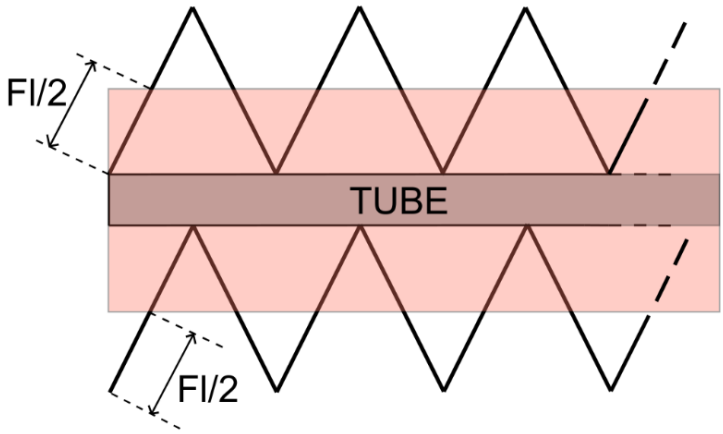

Figure 6. Reduced volume scheme of the study case.

At this point, it has been presented the methodology used to solve the problem, but ε-NTU has some disadvantages that can be overcame. As commented previously, the thermos-physical properties of the fluids are considered constant all along the heat exchanger, and the heat transfer coefficients also have a unique mean value. With the aim of solving this handicap, multi ε-NTU is implemented, and it consists of applying the simple ε-NTU methodology to multiple control volumes. By this, the thermos-physical properties of the fluids and heat transfer coefficients are going to be constant just for a concrete volume control but not for the whole heat exchanger. The implementation of the multi ε-NTU is also needed to take into account the variation or Reynolds and Prandtl number as the coolant advances through the tube, as well as the effect of fluid development which can significantly affect the calculation of the Nusselt number. Figure 7 shows the unique control volume for the whole heat exchanger that corresponds to applying the simple ε-NTU, while Figure 8 shows the total domain discretized in four different control volumes, which corresponds to the multi ε-NTU.

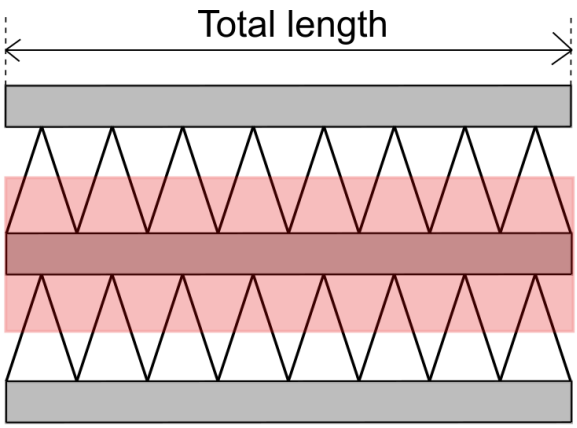

Figure 7. Simple ε-NTU control volume scheme.

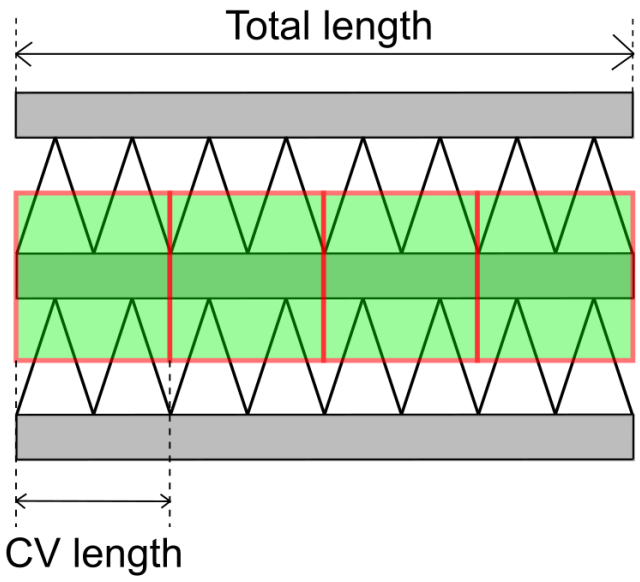

Figure 8. Multi- ε-NTU with four CVs scheme.

3.1.2. Variables calculations

In order to apply the multi ε-NTU method, different variables and thermal properties have to be calculated. In this subsection it is explained how to calculate these variables.

3.1.2.1. Thermal properties of fluids

Thermo-physical properties have been calculated by using Coolprop Library [39], which is able to return a certain thermo-physical property given two known conditions, such as for example temperature and pressure. The fluids thermos-physical properties needed to solve the problem are the following ones:

- Air: $\mu_{air}, \rho_{air}, \lambda_{air}, Cp_{air}$
- Coolant: $\mu_{liq}, \rho_{liq}, \lambda_{liq}, Cp_{liq}$

3.1.2.2. Air variables calculations

The air side calculations needed are the following ones:

- Air velocity: $V_{air} = \frac{\dot{m}_{air}}{\rho_{air} * S_{air}}$

(6)

- Air Reynolds number for louver pitch: $Re_{air,Lp} = \frac{\rho_{air} * V_{air} * Lp}{\mu_{air}}$

(7)

- Air Reynolds number for hydraulic diameter: $Re_{air,Dh} = \frac{\rho_{air} * V_{air} * Dh_{air}}{\mu_{air}}$

(8)

- Air Prandtl number: $Pr_{air} = \frac{\mu_{air} * Cp_{air}}{\lambda_{air}}$

(9)

- Colburn coefficient [30]: $j_{air} = Re_{air,Lp}^{-0,49} * \left(\frac{\theta}{90}\right)^{0,27} * \left(\frac{Fp}{Lp}\right)^{-0,14} * \left(\frac{Fl}{Lp}\right)^{-0,29} * \left(\frac{Td}{Lp}\right)^{-0,23} * \left(\frac{Ll}{Lp}\right)^{0,68} * \left(\frac{Tp}{Lp}\right)^{-0,28} * \left(\frac{Ft}{Lp}\right)^{-0,05}$

(10)

This Colburn coefficient expression was presented by Chang, Hsu, Lin, Wang (1996) [30], and was especially obtained for corrugated fin geometries. Comparing with experimental data, they demonstrated that 89,3% of the data were correlated within ±15% with mean deviation of 7,55%.

- Nusselt number: $Nu_{air} = j_{air} * Re_{air} * (Pr_{air})^{\frac{1}{3}}$

(11)

- Air heat transfer coefficient: $\alpha_{air} = \frac{Nu_{air} * \lambda_{air}}{Dh_{air}}$

(12)

- Air friction factor [29]: $f_{air} = f_1 * f_2 * f_3$

(13)

$$f_1 = 4{,}97 * \left(Re_{air,Lp}\right)^{0{,}6049 - \frac{1{,}064}{\theta^{0,2}}} * \left(ln\left(\left(\frac{Ft}{Fp}\right)^{0,5} + 0{,}9\right)\right)^{-0{,}527}$$

(14)

$$f_2 = \left(\left({}^{Dh}/_{Lp}\right) * \ln\left(0{,}3 * Re_{air,Lp}\right)\right)^{-2{,}966} * \left(\frac{Fp}{Ll}\right)^{-0{,}7931*(Tp/Th)}$$

(15)

$$f_3 = \left(\frac{Tp}{Dm}\right)^{-0{,}0446} * \ln\left(1{,}2 + \left(\frac{Lp}{Fp}\right)^{1{,}4}\right)^{-3{,}553} * \theta^{-0{,}477}$$

(16)

This friction factor expression was presented by Chang, Hsu, Lin and Wang (1999) [29] for this type of radiators geometry. Chang et al compared this correlation with experimentally obtained data and it was shown that 83,14% of the data were correlated within ±15%, and with a mean deviation of 9,21%.

- Air side shear stress:

$$\tau_{air} = \frac{f_{air} * \rho_{air} * {V_{air}}^2}{2}$$

(17)

3.1.2.3. Coolant variable calculations

Analogously to air side calculations, the coolant side calculations are the ones that follow:

- Coolant velocity: $V_{liq} = \frac{\dot{m}_{liq}}{\rho_{liq} * S_{liq}}$

(18)

- Coolant Reynolds number for hydraulic diameter: $Re_{liq,Dh} = \frac{\rho_{liq} * V_{liq} * Dh_{liq}}{\mu_{liq}}$

(19)

- Coolant Prandtl number: $Pr_{liq} = \frac{\mu_{liq} * Cp_{liq}}{\lambda_{liq}}$

(20)

- Coolant Nusselt number:
  2 different formulations have been considered for the calculation of the Nusselt number:

1. Rectangular tube + Gnielinski assumption [40]:

   - If $Re_{liq,Dh} < 3000$:

$$Nu_{liq} = 7{,}54$$

(21)

   - If $Re_{liq,Dh} > 3000$:

$$Nu_{liq} = \frac{\left({}^{f}/_{8}\right) * \left(Re_{liq,Dh} - 1000\right) * Pr_{liq}}{1 + 12{,}7 * \left({}^{f}/_{8}\right)^{0{,}5} * \left(Pr_{liq}{}^{2}/_{3} - 1\right)}$$

(22)

Where $f = \left(0{,}79 * ln\left(Re_{liq,Dh}\right) - 1{,}64\right)^{-2}$

(23)

2. Garimella et al (2001) [31] Nu correlation:

$$Nu_{fd} = 8{,}235 * (1 - 2{,}0421\alpha + 3{,}0853\alpha^2 - 2{,}4765\alpha^3 + 1{,}0578\alpha^4 - 0{,}1861\alpha^5)$$

(24)

Where $\alpha = \frac{Di}{Td-Dm}$

(25)

$$\overline{Nu}_{lam} = \left(Nu_{fd}{}^{3} + \left\{ \frac{0{,}468 * {}^{Dh}/_{L} * Re_{liq,Dh} * Pr_{liq}}{1 + 0{,}165 * \left[{}^{Dh}/_{L} * Re_{liq,Dh} * Pr_{liq}\right]^{2/3}} \right\}^{3} \right)^{1/3} * \left(\frac{\mu_{liq}}{\mu_{liq,wall}} \right)^{0{,}25}$$

(26)

$$\overline{Nu}_{turb} = 0{,}012 * Re_{liq,Dh}{}^{0{,}85} * Pr_{liq}{}^{0{,}4} * \left[1 + \left(\frac{Dh}{L}\right)^{2/3}\right] * \left(\frac{\mu_{liq}}{\mu_{liq,wall}} \right)^{0{,}25}$$

(27)

$$\overline{Nu}_{liq} = \left(\overline{Nu}_{lam}{}^{10} + \left\{ \frac{\exp\left(\frac{360 - Re_{liq,Dh}}{925}\right)}{\overline{Nu}_{lam}{}^{2}} + \frac{1}{\overline{Nu}_{turb}{}^{2}} \right\}^{-5} \right)^{0,1}$$

(28)

This correlation was presented by Garimella, Dowling, Van Der Veen and Killion (2001) [31] and was specially thought for rectangular tubes, typical in automotive heat exchangers, and taking into account the effect of developing flow.

It is important to notate that for Garimella equation, Nusselt number is defined as mean Nusselt number for a given length, for this reason, as in the simulation the domain is discretized in different control volumes, it is needed the calculus of local Nusselt number for the specific control volume. Thus, the local Nusselt number calculation is the following one:

$$Nu_{liq,local} = \frac{\overline{Nu}_{liq}(L2) * L2 - \overline{Nu}_{liq}(L1) * L1}{L2 - L1}$$

(29)

Where $L1$ is the position where control volume starts, and $L2$ is the position where control volume ends.

- Coolant heat transfer coefficient:

$$\alpha_{liq} = \frac{Nu_{liq} * \lambda_{liq}}{Dh_{liq}}$$

(30)

- Coolant friction factor:

1. Rectangular tubes friction factor [40] if $Re_{Dh,liq} < 3000$

$$f_{liq} = 21{,}25 * \left(Re_{liq,Dh}\right)^{-1}$$

(31)

2. Petukhov friction factor if $Re_{Dh,liq} > 3000$

$$f_{liq} = (0{,}79 * \ln\left(Re_{Dh,liq}\right) - 1{,}64)^{-2}$$

(32)

- Coolant side shear stress:

$$\tau_{liq} = \frac{f_{liq} * \rho_{liq} * {V_{liq}}^2}{2}$$

(33)

3.1.2.4. Fin efficiency calculation

Another parameter needed is the fin efficiency, and for this study case in which fins are rectangular and are considered to have an adiabatic extreme, fin efficiency is defined as:

$$\eta_f = \frac{\tanh\left(m_f * {Fl}/{2}\right)}{m_f * {Fl}/{2}}$$

(34)

Where, $m_f = \sqrt{\frac{2*\alpha_{air}}{\lambda_f * Ft}}$

(35)

Another used parameter related with fin efficiency is the surface efficiency defined as:

$$\eta_0' = \frac{A_{air,nf} + \eta_f A_{air,f}}{A_{air}}$$

(36)

3.1.2.5. Overall heat transfer coefficient calculation

The overall heat transfer coefficient has an important role in heat exchangers studies, and so it is in this study case. It is going to be used for the calculation of the total heat transfer rate, and it contains the information related with the different thermal resistances existing. As it can be seen in the scheme of

Figure 9, the thermal resistances in the study case are the convection on the air side surface, the conduction through the metallic tube thickness, and the convection on the coolant side surface. For this simulation, it has been chosen that the overall heat transfer coefficient is associated to the air heat transfer surface.

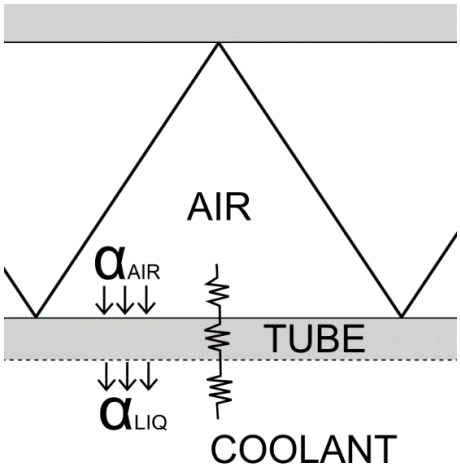

Figure 9. Scheme of thermal resistances of the radiator.

Thus, the overall heat transfer coefficient expression is:

$$U = \left[\frac{1}{\alpha_{air}}\frac{A_{air}}{A_{liq}} + \frac{Tt}{\lambda t}\frac{A_{air}}{A_{liq}} + \frac{1}{\alpha_{air}\eta_0'}\right]^{-1}$$

(37)

3.1.2.6. Heat transfer rate calculation

The heat transfer is calculated following the ε-NTU methodology, so its formulation is:

$$\dot{Q} = \varepsilon\,(\dot{m} * Cp)_{min} * (T_{air,in} - T_{liq,in})$$

(38)

3.1.3. Algorithm Structure

3.1.3.1. Main structure

Before commenting the algorithm structure, it is important to remember that the study focuses on only one of the tubes of the radiator, and half of the upper fins and half of the under fins. Another relevant aspect to take into account is that the methodology applied is

the multi ε-NTU, which means that the domain is discretized in smaller control volumes, and this will directly affect the algorithm structure. To have a clearer idea on how the code works, it is presented the summarized algorithm structure used to solve the problem.

- Introduction of geometric parameters and simulation parameters.
- Previous calculations
- Introduction of inlet conditions
- "For" loop that goes through control volume by control volume, from 1 to N.
    1. "While" loop used to find the outlet conditions for a particular control volume, and which terminates when these outlet conditions have been found.
    2. End of "While" loop.
- End of "For" loop.
- Obtention of results.

3.1.3.2. Detailed procedure

Following the main structure already presented, now a more detailed explanation of the code implementation is explained.

1. Geometric and numeric parameters and working conditions

Introduction of all the already known geometric parameters:
$Lp, \theta, Fp, Ft, Fd, Td, Tt, Tp, Th, L_{total}, N_{tubes}$.

Introduction of inlet fluid conditions are and total flow rates:
$T_{air,in}, T_{liq,in}, P_{air,in}, P_{liq,in}, \dot{m}_{air,total}, \dot{m}_{liq,total}$.

Introduction of aluminum thermal conductivity: λ_t, λ_{fin}

Introduction of numeric parameters such as relaxation factor, number of control volumes and convergence criteria value: fr, N, δ

2. Previous calculations

$\dot{m}_{liq}$ is calculated using (64)

$\dot{m}_{air}$ is calculated using (65)

L is calculated using (66)

N_{fins} is calculated using (67)

Lh is calculated using (68)

Dm is calculated using (69)

Di is calculated using (70)

Ts is calculated using (71)

Fl is calculated using (72)

Ll is calculated using (73)

S_{air} is calculated using (54)

Per_{air} is calculated using (55)

S_{liq} is calculated using (56)

Per_{liq} is calculated using (57)

A_{liq} is calculated using (60)

Dh_{liq} is calculated using (58)

$A_{air,nf}$ is calculated using (61)

$A_{air,f}$ is calculated using (62)

A_{air} is calculated using (63)

Dh_{air} is calculated using (59)

3. Initialization of coolant temperature and coolant pressure vectors

These vectors are called P_{liq} and T_{liq} , and will have N+1 dimension. Its size increases during the simulation. Their components are the values of pressure and temperature, respectively, of the inlet and outlet of each control volume. Thus, for example, the k component of the vector is the outlet value of the k-1 control volume, and the inlet value of the k control volume.

4. "For" loop that visits control volume by control volume from k=1 to N

This loop visits control volume by control volume. It does not change onto the next control volume until the ε-NTU has been applied to the present control volume and the outlet

conditions of the present control volume are known.

- Using Coolprop, it is calculated the $\rho_{air,in}$ and $\rho_{liq,in}$ values, as inlet temperatures and pressures are known.
- $V_{air,in}$ and $V_{liq,in}$ are calculated using (6)
- $T_{air,out}$,$T_{liq,out,}$,$P_{air,out}$$P_{liq,out}$, $T_{air,wall}$ $T_{liq,wall}$ are needed to proceed the calculations in the control volume, so they are initialized as:
  - $T_{air,out} = T_{air,in}$
  - $T_{liq,out} = T_{liq,in}$
  - $P_{air,out} = P_{air,in}$
  - $P_{liq,out} = P_{liq,in}$
  - $T_{air,wall} = T_{air,in}$
  - $T_{liq,wall} = T_{liq,in}$

  In this way, initially the outlet values are the same as the inlet values, although they will be recalculated iteratively.

4.1. "While" loop that applies the ε-NTU methodology

This loop applies the ε-NTU methodology in order to solve the thermal problem in the present control volume. In this way, the code applies the ε-NTU iteratively, until the obtained values converge, according to a convergence criteria.

- Calculation of mean values of temperature and pressure, for air and coolant:
  - $T_{air,mean} = \frac{T_{air,in}+T_{air,out}}{2}$
  - $T_{liq,mean} = \frac{T_{liq,in}+T_{liq,out}}{2}$
  - $P_{air,mean} = \frac{P_{air,in}+P_{air,out}}{2}$
  - $P_{liq,mean} = \frac{P_{liq,in}+P_{liq,out}}{2}$

- Using Coolprop, it is calculated the $\rho_{air,out}$ and $\rho_{liq,out}$ values.
- Calculation of fluids outlet velocities $V_{air,out}$ and $V_{liq,out}$ using (6)
- The mean air properties μ_{air}, Cp_{air}, ρ_{air}, λ_{air} are calculated using Coolprop, at $T_{air,mean}$ and $P_{air,mean}$.
- The mean coolant properties μ_{liq}, Cp_{liq}, ρ_{liq}, λ_{liq} are calculated using Coolprop, at $T_{liq,mean}$ and $P_{liq,mean}$.
- The $\mu_{liq,wall}$ is calculated using Coolprop, at $T_{liq,wall}$ and $P_{liq,mean}$.
- Calculation of fluids mean velocities $V_{air,mean}$ and $V_{liq,mean}$.

- Air side calculations:
  - $Re_{air,Lp}$ using (7)
  - $Re_{air,Dh}$ using (8)
  - Pr_{air} using (9)
  - j_{air} using (10)
  - Nu_{air} using (11)
  - α_{air} using (12)
  - f_{air} using (13)
  - τ_{air} using (17)

- Coolant side calculations:
  - $Re_{liq,Dh}$ using (19)
  - Pr_{liq} using (20)
  - f_{liq} using (31)
  - τ_{liq} using (33)
  - Nu_{liq} using (21), (22) or (29)
  - α_{liq} using (30)

- Calculation of fin efficiency parameters:
  - m_f using (35)
  - η_f using (34)
  - η_0' using (36)

- Calculation of the overall heat transfer coefficient U, referred to the air heat transfer surface A_{air}, using (37)

- Calculation of ε-NTU parameters:
  - $C_{min} = \min(\dot{m}_{liq}Cp_{liq}, \dot{m}_{air}Cp_{air})$

(39)

  - $C_{max} = \max(\dot{m}_{liq}Cp_{liq}, \dot{m}_{air}Cp_{air})$

(40)

- NTU using (3)
- Z using (4)
- ε using (5)
- $\dot{Q}$ using (1) and (2)

- Recalculate outlet and wall conditions

  At this point, the initially supposed values, $T_{air,out}$, $T_{liq,out}$, $P_{air,out}$, $P_{liq,out}$, $T_{liq,wall}$ and $T_{air,wall}$, are recalculated for the next iteration in the "while" loop. The recalculation of these values is made from the $\dot{Q}$ obtained, and its expressions are the following ones:

  - $$T_{liq,out}^{new} = T_{liq,in} + \dot{Q} \Big/ (\dot{m}_{liq} * Cp_{liq})$$

    (41)

  - $$T_{air,out}^{new} = T_{air,in} - \dot{Q} \Big/ (\dot{m}_{air} * Cp_{air})$$

    (42)

  - $$P_{liq,out}^{new} = P_{liq,in} - \frac{(\dot{m}_{liq} * (V_{liq,out} - V_{liq,in}) + \tau_{liq} * Per_{liq} * L)}{S_{liq}}$$

    (43)

  - $$P_{air,out}^{new} = P_{air,in} - \frac{(\dot{m}_{air} * (V_{air,out} - V_{air,in}) + \tau_{air} * A_{air})}{S_{air}}$$

    (44)

  - $$T_{liq,wall}^{new} = T_{liq,mean} + \dot{Q} \Big/ (A_{liq} * \alpha_{liq})$$

    (45)

  - $$T_{air,wall}^{new} = T_{air,mean} - \dot{Q} \Big/ (A_{air} * \eta_0' * \alpha_{air})$$

    (46)

- Comparison of new obtained values with the previous ones:
  It is calculated a new parameter called "a", which is the maximum difference between the recalculated value and the previous one, of all six variables:

- $a = \max\{abs[(T_{liq,out}^{new} - T_{liq,out}), (T_{air,out}^{new} - T_{air,out}), (P_{liq,out}^{new} - P_{liq,out}), (P_{air,out}^{new} - P_{air,out}), (T_{liq,wall}^{new} - T_{liq,wall}), (T_{air,wall}^{new} - T_{air,wall})]\}$

(47)

- New values for the next iteration are calculated
  The new values of $T_{air,out}$, $T_{liq,out}$, $P_{air,out}$, $P_{liq,out}$, $T_{liq,wall}$ and $T_{air,wall}$ for the next iteration are obtained by applying a relaxation factor, fr:

  - $T_{liq,out}^{next\ iter} = T_{liq,out} + fr * (T_{liq,out}^{new} - T_{liq,out})$

  (48)

  - $T_{air,out}^{next\ iter} = T_{air,out} + fr * (T_{air,out}^{new} - T_{air,out})$

  (49)

  - $P_{liq,out}^{next\ iter} = P_{liq,out} + fr * (P_{liq,out}^{new} - P_{liq,out})$

  (50)

  - $P_{air,out}^{next\ iter} = P_{air,out} + fr * (P_{air,out}^{new} - P_{air,out})$

  (51)

  - $T_{liq,wall}^{next\ iter} = T_{liq,wall} + fr * (T_{liq,wall}^{new} - T_{liq,wall})$

  (52)

  - $T_{air,wall}^{next\ iter} = T_{air,wall} + fr * (T_{air,wall}^{new} - T_{air,wall})$

  (53)

4.2. End of "While" loop

At the end of each iteration of the "while" loop, the value of a obtained in (47) and is compared with δ, which is the convergence criteria value. If $a > \delta$, convergence is not reached yet, so another iteration in the "while" loop starts again, with the values of temperature and pressure obtained from (48) to (53). If $a < \delta$, it is considered that convergence has been reached, so the "while" loop ends, and the outlet temperatures and pressures will be used as the inlet temperature and pressures of the next control volume.

5. Update of data vectors

In order to save the data obtained from applying the ε-NTU at the last studied control volume, the pressure and temperature vectors are updated with the values obtained at the end of the "while" loop. These vectors are also used in the next iteration of the "for" loop, as they will be used for the inlet value of the next control volume. Moreover, at the end of the simulation it will be possible to see the temperature and pressure distributions along the heat exchanger. In the same way it is done for pressures and temperatures, other vectors can be created to save the data of interesting variables such as α, $\dot{Q}$, or Reynolds number, between others.

$$T_{air}(k) = T_{air,out}$$

$$P_{air}(k) = P_{air,out}$$

$$T_{liq}(k+1) = T_{liq,out}$$

$$P_{liq}(k+1) = P_{liq,out}$$

6. End of "for" loop

The end of "for" loop occurs when k=N, which is the last control volume of the tube of the radiator. It is the end of the iterative process of the code, and the calculations are over.

7. Results

This is the last part of the algorithm and consists on printing the results that are wanted to be seen. It is possible to see the evolution control volume by control volume of the outlet air temperature, the fluid temperature, the heat transfer rate, the heat transfer coefficients or any variable wanted.

3.2. Study Case

At this point, the methodology and the algorithm to apply it have been explained. This section aims to define the study case that is going to be simulated. The simulation carried out in this project is on a typical aluminum automotive radiator. These radiators have usually louvered fins, in order to increase its thermal performance and reduce as much as possible their dimensions, which is especially important in a car design. The heat exchange occurs between the outside air, present in the atmosphere, and a liquid coolant that circulates through the tubes of the radiator.

3.2.1. Appearance and working principle

Vehicle radiators are cross-flow heat exchangers, and their typical appearance consist on having triangular channels for the air flow, and flat tubes for the liquid or coolant flow, as it can be seen in Figure 10 and Figure 11. Furthermore, it can also be seen that the triangular channels are louvered in order to increase the heat transfer rate between the two fluids.

Its operation is based on atmosphere air that enters to the triangular channels, and comes out of these channels at a lower or higher temperature due to the heat transferred or acquired from the coolant.

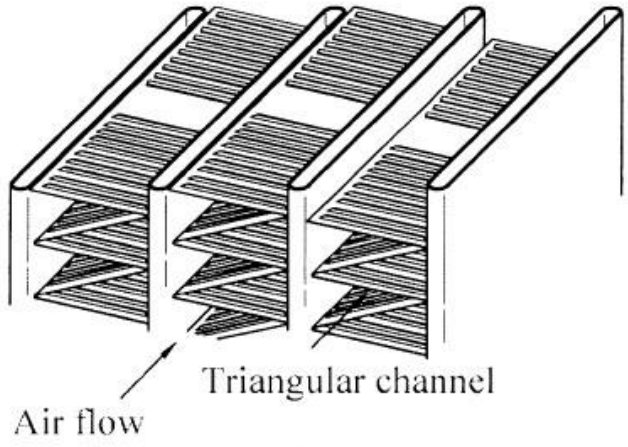

Figure 10. Appearance and geometry of the study case radiator. [30]

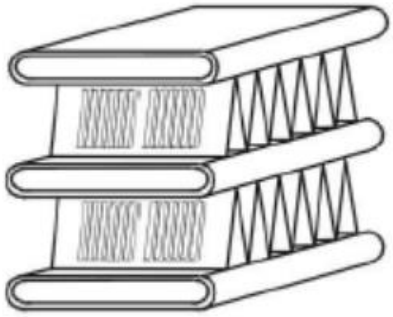

Figure 11. Appearance and geometry of the study case radiator. [41]

3.2.2. Fluids involved

The aim of the heat exchanger of this study case is to have an optimal heat transfer rate, and it also depends on the fluids that circulate inside. For a car radiator, one of the fluids is the air that comes from the outside, as it is very easy to obtain from the atmosphere. The other fluid is the liquid coolant, and for this study two options have been considered. One is ethylene glycol and water at 50% in mass, which is a typical anti-freezing liquid for this kind of applications, and the other coolant considered is pure water.

3.2.3. Working conditions

As said before, the radiator can basically work in two different configurations. On one hand, it can be the liquid that enters the radiator at a higher temperature than air, and it gets cooler by transferring heat to the air. On the other hand, it can work as the liquid that enters at a lower temperature than air, and gets hotter as it acquires heat from the outside air. For the first case, the coolant enters at near 90ºC, while for the second case the coolant enters near 15ºC. It is well known that the typical working conditions are that the liquid is cooled down, nevertheless, in simulations that will be seen later, it operates with cold liquid. It has to be taken into account for the inlet conditions that the inlet air is coming from the atmosphere. Regarding the inlet pressure of the coolant, a typical value is near 1,5 atmospheres.

In terms of mass flow rates of the two fluids involved, it has been decided to work with different values of air mass flow in order to have a more realistic simulation, as the air mass flow depends on the velocity in which the vehicle is moving. For the liquid mass flow, it has also been decided to work with different values. More concretely, the values of mass flow rates are ranged between the following values:

Air: range between 0,08 Kg/s and 0,39 Kg/s.

Liquid: range between 500 Kg/h and 2500 Kg/h.

At this point, it has been defined the working conditions of the radiator in a general way,

nevertheless, in all situations discussed below, the working conditions will be concretely specified.

3.2.4. Geometry

As it has been commented before, the geometry consists on triangular channels where the air goes through, and flat tubes for the coolant, in a way that air and coolant flow in perpendicular directions.

3.2.4.1. Global dimensions

In Figure 12 it is shown a global sketch of the radiator. It is composed of 12 flat tubes, and each of these tubes has upper and lower fins, precisely these fins form the triangular channels through which the air flows.

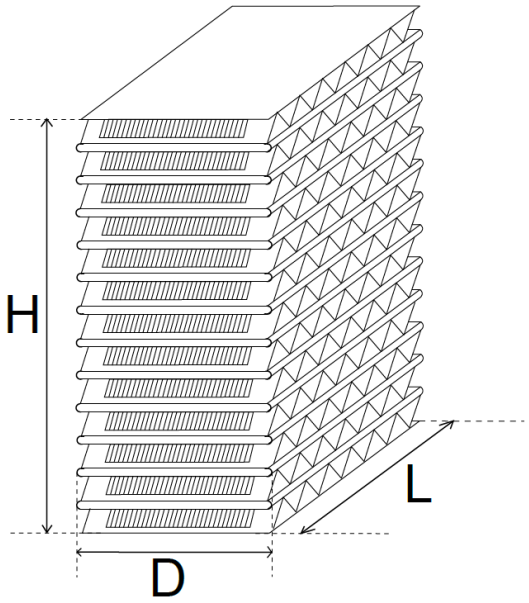

Figure 12. Scheme of the whole heat exchanger

The global dimensions of the heat exchanger are:

- Total height: $H = 0{,}133\ m$
- Total depth: $D = 0{,}023\ m$
- Total finned length: $L_{total} = 0{,}184\ m$

3.2.4.2. Known geometric parameters

To go into detail on the geometry, it is necessary to present the geometrical parameters that conform the radiator, which are the following ones:

- Fin thickness: $Ft = 0{,}0001\ m$
- Fin pitch: $Fp = 0{,}00119\ m$
- Fin depth: $Fd = 0{,}023\ m$
- Tube thickness: $Tt = 0{,}00032\ m$
- Tube depth: $Td = 0{,}023\ m$
- Tube pitch: $Tp = 0{,}0104\ m$
- Tube height: $Th = 0{,}0021\ m$
- Louver pitch: $Lp = 0{,}0009\ m$
- Louver angle: $\theta = 26º$
- Total length: $L_{total} = 0{,}184\ m$
- Number of tubes: $N_{tubes} = 12$

3.2.4.3. Air Section

As it has been explained in part 3.1.1, this simulation focuses in only one tube. Due to that, the air section geometry is analyzed just for half of the upper fins of the tube and half of the lower fins, and only for a length of a fin pitch, as the geometry is repeated every fin pitch. The scheme of the air section is the one in Figure 13.

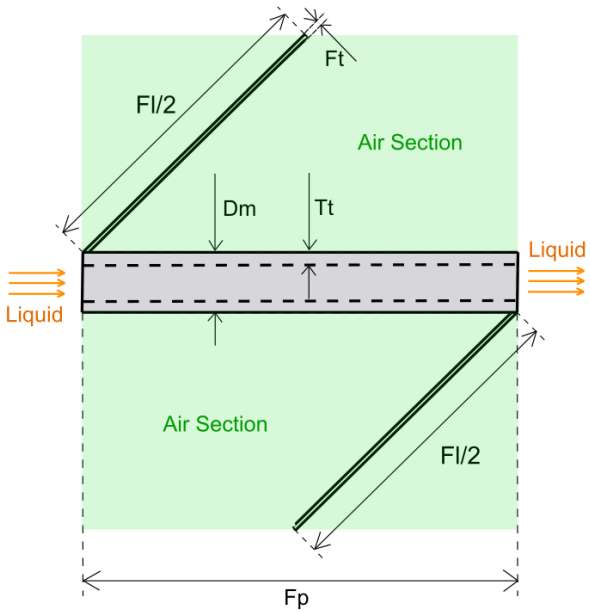

Figure 13. Air section geometry.

As from air section geometry, the section and the perimeter can be calculated as:

- Air section: $S_{air} = (F_p * T_s - 2 * \frac{F_l}{2} * F_t) * N_{fins}$

(54)

- Air perimeter: $Per_{air} = \left(2 * \left(\frac{Fl}{2} * 2 + Fp\right)\right) * N_{fins}$

(55)

3.2.4.4. Coolant section

The coolant section geometry can be seen in Figure 14. The flat tubes and the fins in between them are defined by some geometric parameters. Figure 14 also shows the geometry of the louvers that are located in the fins.

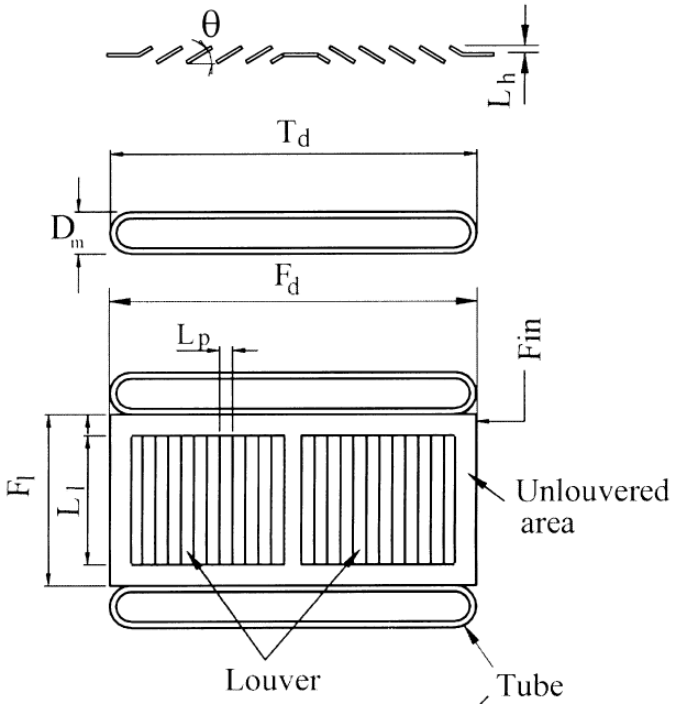

Figure 14. Coolant section geometry and louvered region geometry. [29]

As from coolant section geometry, the section and the perimeter can be calculated as:

- Liquid section: $S_{liq} = (Td - Dm) * Di + \pi * \frac{Di^2}{4}$

(56)

- Liquid perimeter: $Per_{liq} = 2 * (Td - Dm) + \pi * Di$

(57)

3.2.4.5. Other geometric calculations

From Figure 13 and Figure 14, other geometric parameters that are needed in the simulation are calculated:

- Liquid section hydraulic diameter: $Dh_{liq} = 4\frac{S_{liq}}{Per_{liq}}$

(58)

- Air section hydraulic diameter: $Dh_{air} = 4 * \frac{S_{air}}{Per_{air}}$

(59)

- Liquid side heat transfer area: $A_{liq} = Fp * Fd * 2 * N_{fins}$

(60)

- Air side non finned heat transfer area: $A_{air,nf} = (Fp - Ft) * Fd * 2 * N_{fins}$

(61)

- Air side finned heat transfer area: $A_{air,f} = 2 * Fl * Fd * N_{fins}$

(62)

- Air side total heat transfer area: $A_{air} = A_{air,nf} + A_{air,f}$

(63)

- Liquid mass flow for a single tube: $\dot{m}_{liq} = {\dot{m}_{liq,total}}/{N_{tubes}}$

(64)

- Air mass flow for a single control volume: $\dot{m}_{air} = {\dot{m}_{air,total}}/{(N_{tubes} * N)}$

(65)

- Length of a single control volume: $L = {L_{total}}/{N}$

(66)

- Number of fins for a single control volume: $N_{fins} = {L}/{Fp}$

(67)

- Louver height: $Lh = \frac{Lp * \tan(\theta)}{2}$

(68)

- External tube diameter: $Dm = Th$

(69)

- Inner tube diameter: $Di = Dm - 2 * Tt$

(70)

- Space between tubes: $Ts = Tp - Th$

(71)

- Fin length: $Fl = \sqrt{Ts^2 + Fp^2}$

(72)

- Louver length: $Ll = 0{,}75 * Fl$

(73)

3.3. Validation of the code

This section aims to validate the model for this project study case, which both have been explained in the previous sections 3.1 and 3.2. It is important to notate that the simulation results cannot be shown in a direct way, in order to not reveal some confidential data that has been used in the project, and which cannot be shown. For this reason, some variables are presented as $X^* = \frac{X_{sim}}{X_{ref}}$, where X is a general studied variable, X_{ref} is an unknown reference value, and X_{sim} is the value obtained in the simulation.

3.3.1. Validation of mesh

For the mesh independence study, it has been plotted the heat transfer rate in function of the number of control volumes, for 4 different cases. In all four cases the inlet temperatures and pressures have been the same, and have been selected arbitrarily, $P_{air,in} = 1\ atm; T_{air,in} = 40ºC; P_{liq,in} = 1{,}5\ atm; T_{liq,in} = 95ºC$. The coolant used in the simulation is ethylene-glycol + water at 50% in mass. The only conditions that change, for each of these cases are the mass flow rates:

- Case 1: $\dot{m}_{liq} = 0{,}14\ kg/s;\ \dot{m}_{air} = 1000\ kg/h$
- Case 2: $\dot{m}_{liq} = 0{,}21\ kg/s;\ \dot{m}_{air} = 1500\ kg/h$
- Case 3: $\dot{m}_{liq} = 0{,}28\ kg/s;\ \dot{m}_{air} = 2000\ kg/h$
- Case 4: $\dot{m}_{liq} = 0{,}39\ kg/s;\ \dot{m}_{air} = 2500\ kg/h$

With these four cases, the results can be seen for typical operational values of air and coolant mass flows.

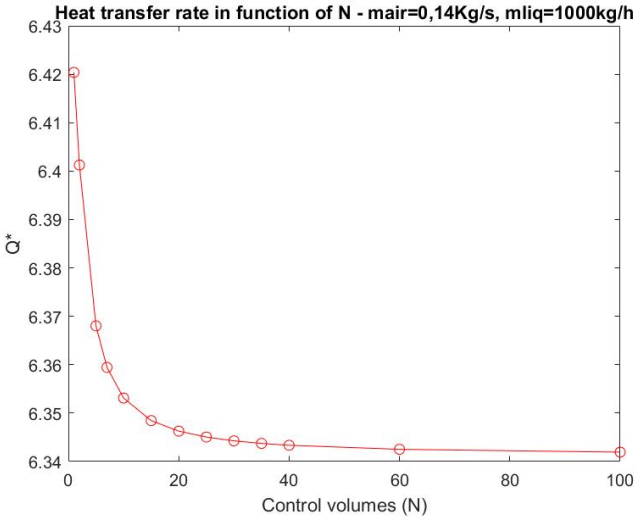

Figure 15. Heat transfer rate in function of N. Case 1

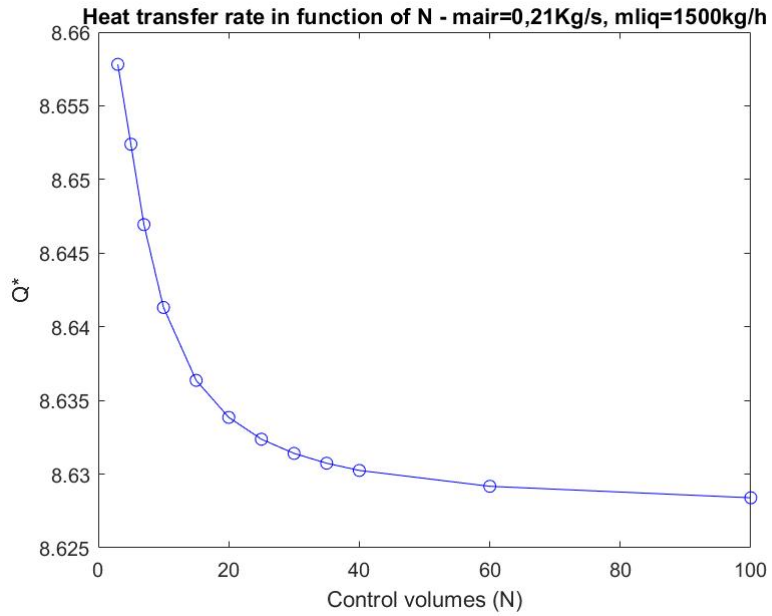

Figure 17. Heat transfer rate in function of N. Case 2

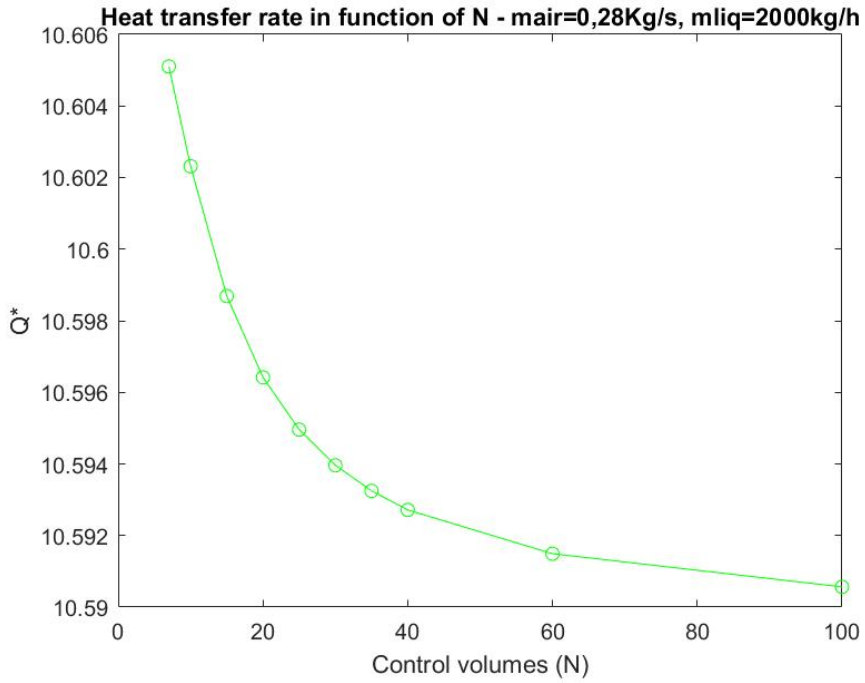

Figure 16. Heat transfer rate in function of N. Case 3

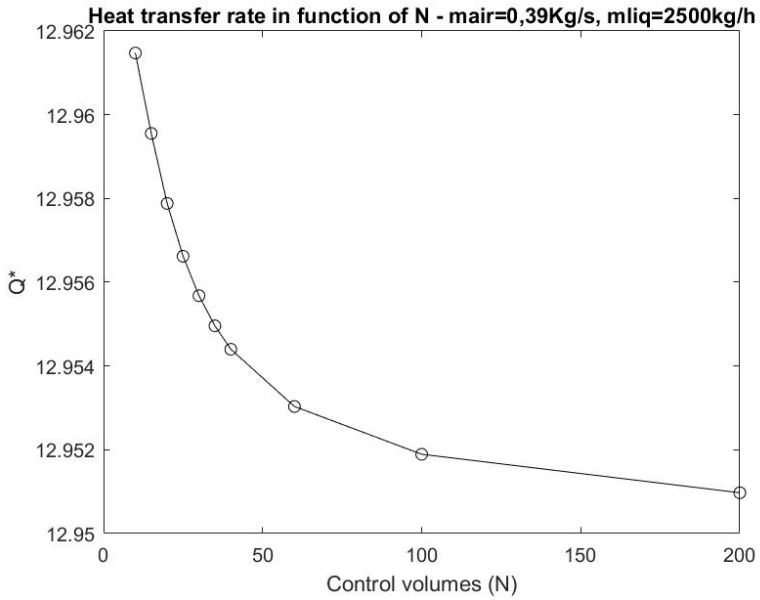

Figure 18. Heat transfer rate in function of N. Case 4

Regarding the results obtained, it has been considered that N=60 is a number of control volumes for which the result has converged enough, and this will be used for next simulations. Visually, it is easy to observe for Figure 15, Figure 17 and Figure 16, that when N=60 the heat transfer rate value is near the converged value. Nevertheless, in Figure 18 it is not so evident, as for N=60 the heat transfer value has still not converged at all, but it also can be seen that there's not too much difference between the converged heat transfer rate value and the heat transfer rate value when N=60, concretely 0,016%, so for this reason it has been considered good enough.

3.3.2. Validation of heat transfer calculation

3.3.2.1. Comparison to experimental results

For the liquid side, two different correlations for heat transfer calculation have been used, corresponding to (21) (rectangular tubes), (22) (Gnielinski) and (29) (Garimella et al [31]), and for the air side heat, Chang and Wang correlation [30] has been applied. At first, it is wanted to see the differences between the two liquid heat transfer correlations used, and to do that, the results have been compared with ones obtained in three experiments. These experiments were part of a previous work carried out as part of an in-company research project in Carles Oliet's doctoral thesis [42].

This experimental data is confidential, and for this reason the results are presented in terms of error, and in some cases, as mentioned before, are calculated over a not given reference value.

The liquid side correlations that have been used are:

1. Rectangular tubes correlation (21) + Gnielinski (22)
    - Rectangular tubes correlation is used when $Re_{liq,Dh} < 3000$
    - Gnielinski correlation is used when $Re_{liq,Dh} > 3000$

2. Garimella et al correlation (24) accepts $Re_{liq,Dh} < 10671$

The first experiment conditions were the following ones:

- Coolant mass flow rates: [1000 Kg/h, 1500 Kg/h, 2000 Kg/h]
- Air mass flow rates: [0,14 Kg/s, 0,21 Kg/s, 0,28 Kg/s, 0,39 Kg/s]
- Inlet conditions: $T_{liq,in} = 15ºC$, $T_{air,in} = 40ºC$, $P_{liq,in} = 1{,}5\ atm$, $P_{air,in} = 1\ atm$
- Coolant: Water

Given these mass flow rates, 12 different cases are analyzed. These inlet conditions indicate that the coolant works at a low temperature, being the fluid that is heated, while the air is the fluid that gets cooler.

The experimental results are confidential data, so they can't be directly shown. Nevertheless, the error can be presented without showing the value. For this reason, it is calculated the error respect the experimental value, defined as it follows:

$$Err = 100 * \frac{(Q_{sim} - Q_{\exp})}{Q_{exp}} \quad (74)$$

The results obtained are the following ones:

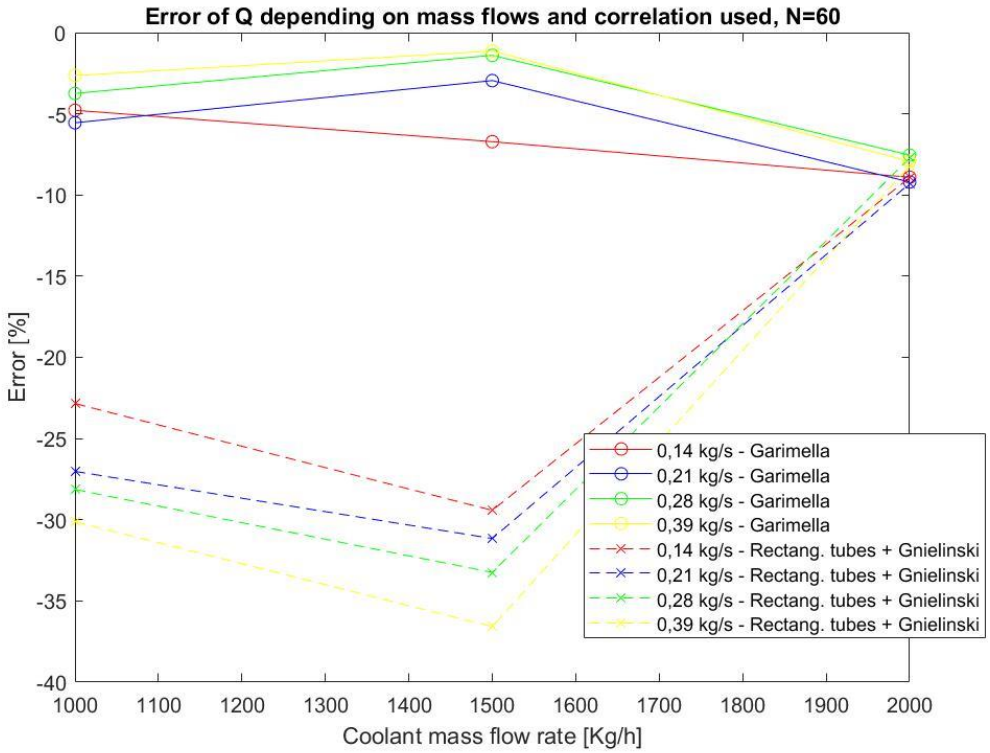

Figure 19. Error of Q depending on mass flows and correlation used. Experiment 1.

In Figure 19 it is represented the % of error of Q respect the experimental results, for when it is calculated using Garimella correlation, and when it is calculated using rectangular tubes + Gnielinski correlation. As it can be seen, The Garimella correlation shows less error than rectangular tubes + Gnielinski correlation. Nevertheless, the difference of error between the two correlations is higher when the coolant flow rate is low, but there is not significant difference of error when the coolant flow is higher. That is probably because for higher Reynolds, Gnielinski equation is used, and it shows a good performance, or at least similar performance to Garimella's correlation, but for low Reynolds, Rectangular tubes correlation is used, which shows a higher error. Garimella correlation shows a better performance, especially for low Reynolds, and the error in all cases I lower than 10%.

For the second experiment conditions were the following ones:

- Coolant mass flow rates: [404 kg/h, 985 kg/h, 2567 kg/h]
- Air mass flow rates: [0,08 kg/s, 0,14 kg/s, 0,21 kg/s, 0,27 kg/s]
- Inlet conditions: $T_{liq,in} = 95ºC$, $T_{air,in} = 27ºC$, $P_{liq,in} = 1{,}5\ atm$, $P_{air,in} = 1\ atm$
- Coolant: Ethylene-glycol + water at 50% in mass

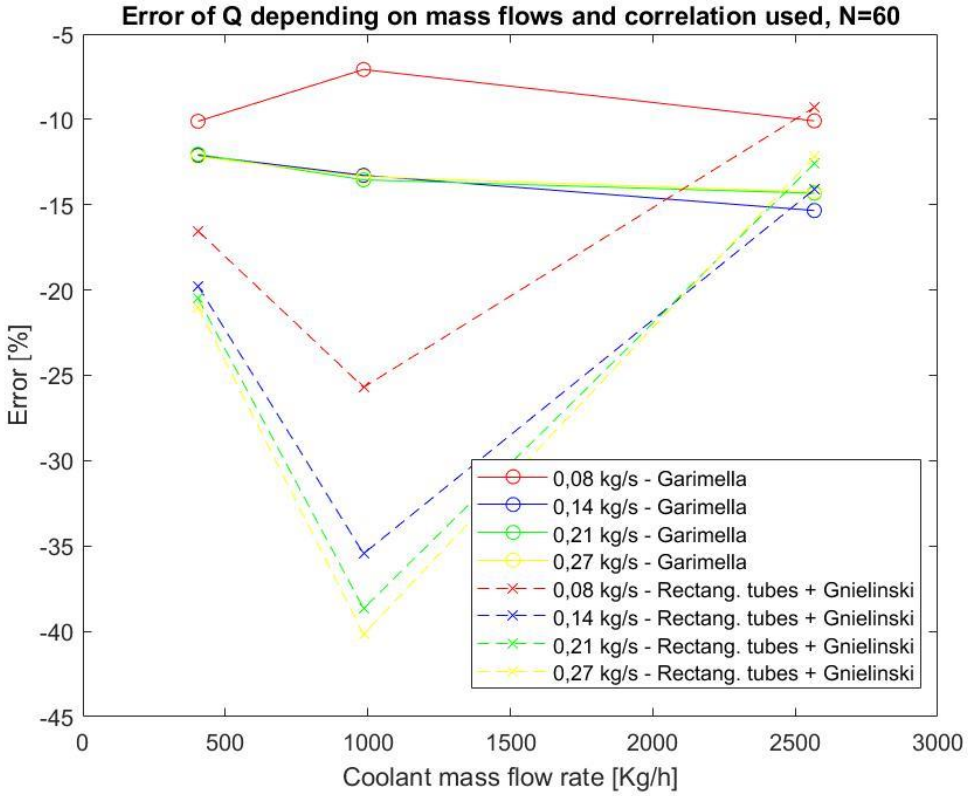

Figure 20. Error of Q depending on mass flows and correlation used. Experiment 2.

Figure 20 shows in the same way as Figure 19 the % of error of Q in function of mass flows and correlation used. It has to be considered that in this case, the working principle has changed respect the first experiment, as in this one it is the coolant that gets cooler, and the air that gets hotter. Nevertheless, the results are similar to the ones obtained in experiment 1. It can be seen that by using Garimella equation the error is ranged between 5% and 15% approximately, and it can also be seen that for low coolant mass flow rates, the rectangular

tubes correlation provides a greater error.

For the third experiment conditions were the following ones:

- Coolant mass flow rates: [404 kg/h, 994 kg/h, 2567 kg/h]
- Air mass flow rates: [0,08 kg/s, 0,14 kg/s, 0,21 kg/s, 0,27 kg/s]
- Inlet conditions: $T_{liq,in} = 95ºC$, $T_{air,in} = 40ºC$, $P_{liq,in} = 1{,}5\ atm$, $P_{air,in} = 1\ atm$
- Coolant: Ethylene-glycol + water at 50% in mass

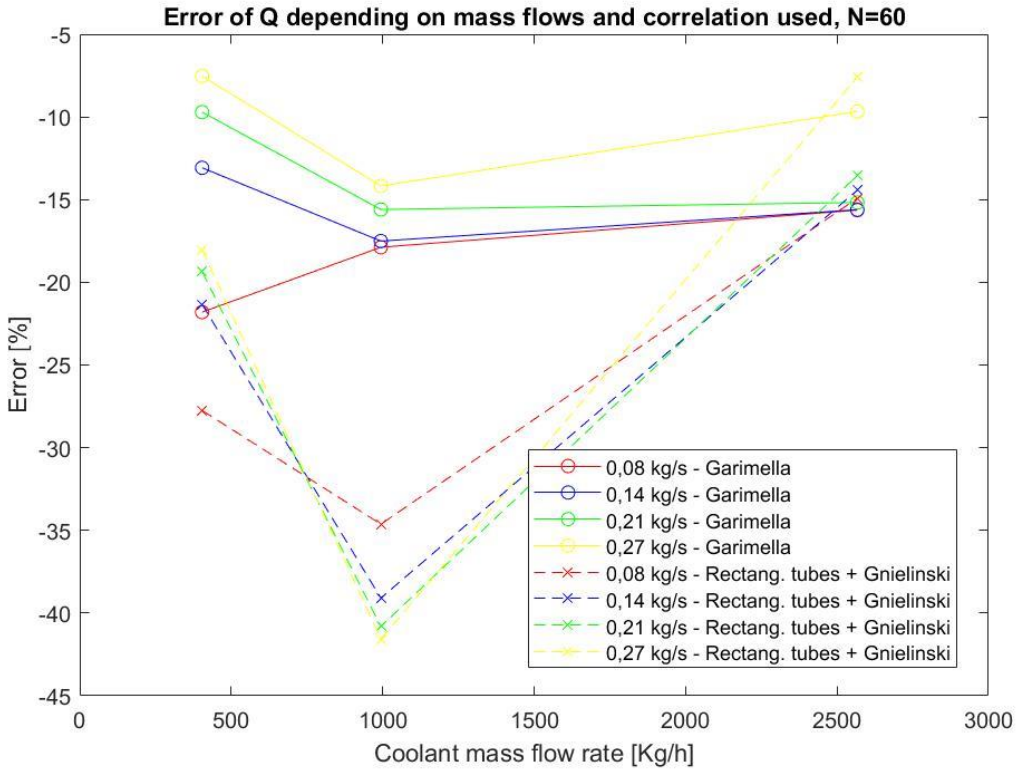

Figure 21. Error of Q depending on mass flows and correlation used. Experiment 3.

In the same line as the second experiment, in this third one the coolant gets cooler and the air is heated, but in this case the inlet temperature is higher. The results obtained are shown in Figure 21 and they are similar to the ones for experiment 1 and 2. It can be seen that Garimella equation provides a less than 20% error, while the rectangular tubes + Gnielinski equation shows higher error, especially for low Reynolds. Thus, similar conclusions are reached when observing Figure 19, Figure 20 and Figure 21, and it can be considered that Garimella equation offers more accurate results.

3.3.2.2. Nusselt vs Reynolds for the two correlations

Beyond the comparison with experimentally obtained results, done in the previous section, it has been plotted the Nusselt – Reynolds graphic to understand better the difference between the two correlations used for heat transfer calculation at liquid side. For this plot, it has been concreted the following variables, which are needed to calculate the Nusselt number, and have coherent values respect the present study case:

- $Pr_{liq} = 8$
- $L_{total} = 0{,}184\ m$
- Rectangular tube ratio $\alpha = 0{,}0698$
- $Dh_{liq} = 2{,}92\ mm$
- $\frac{\mu}{\mu_{wall}} = 1/3$

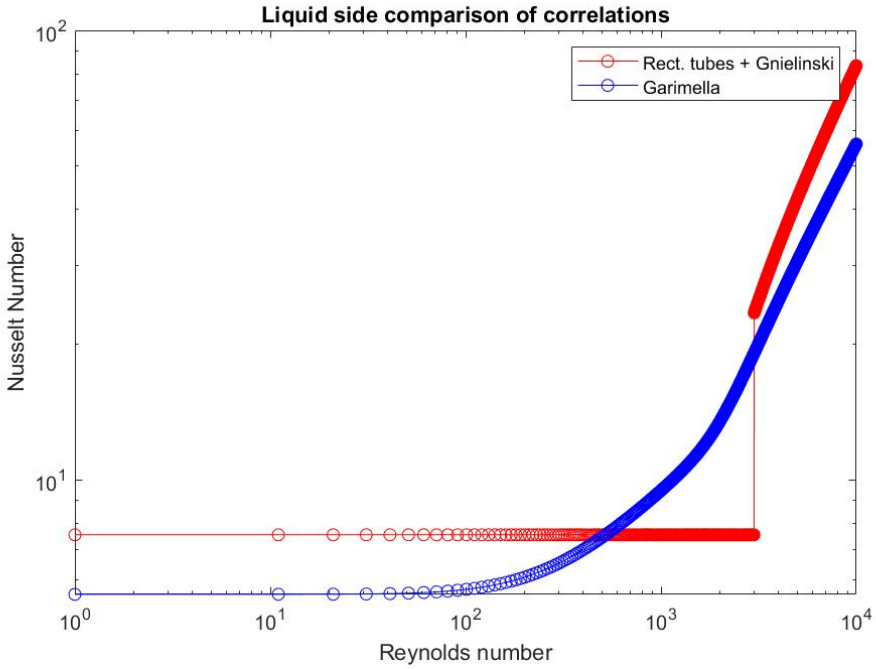

Figure 22. Nusselt vs Reynolds plot, for the two liquid side heat transfer correlations used.

It can be seen in Figure 22, that the Garimella equation has defined a continuous correlation in the transition zone from laminar to turbulent regime. This correlation was obtained especially for flat tubes of vehicle radiators, what makes it more suitable for this study case. It also can be observed that the rectangular tubes + Gnielinski correlation has a notable discontinuity when $Re_{liq} = 3000$, as rectangular tubes correlation is thought for laminar flow, and Gnielinski for turbulent flow, but there's no consideration for a transition zone. This is consistent with the results showed in Figure 19 and Figure 21, where it is seen that for higher coolant mass flows, the Reynolds number of liquid is higher, and Gnielinski equation shows a

similar performance to Garimella equation, but for low coolant mass flows, Reynolds number is lower, and rectangular tubes correlation is not good enough to predict the heat transfer.

It is important to notate that Garimella equation is defined for a ratio of viscosities $\frac{\mu_{liq}}{\mu_{liq,wall}}$ ranged between 0,243 and 0,630, but it is not possible to achieve when the coolant enters at lower temperature than air. For this reason, Garimella correlation is especially thought for applications in which coolant enters the radiator at higher temperatures than air.

3.3.2.3. Q vs Reynolds for the two correlations

Following in the same line as the previous section, it also has been analyzed the different behavior between the two used correlations by presenting a plot of heat transfer rate versus liquid Reynolds. The simulation conditions to obtain this plot are the following ones:

- $T_{air,in} = 40ºC;\ P_{air,in} = 1\ atm\ ;\ T_{liq,in} = 95ºC;\ P_{liq,in} = 1{,}5\ atm$
- $\dot{m}_{liq}$ varies between 1000 kg/h and 2500 kg/h
- $\dot{m}_{air}$ constant at 0,28 kg/s

Two different plots are obtained, one corresponding to the use of water as coolant, and the other corresponding to the use of ethylene glycol + water as coolant:

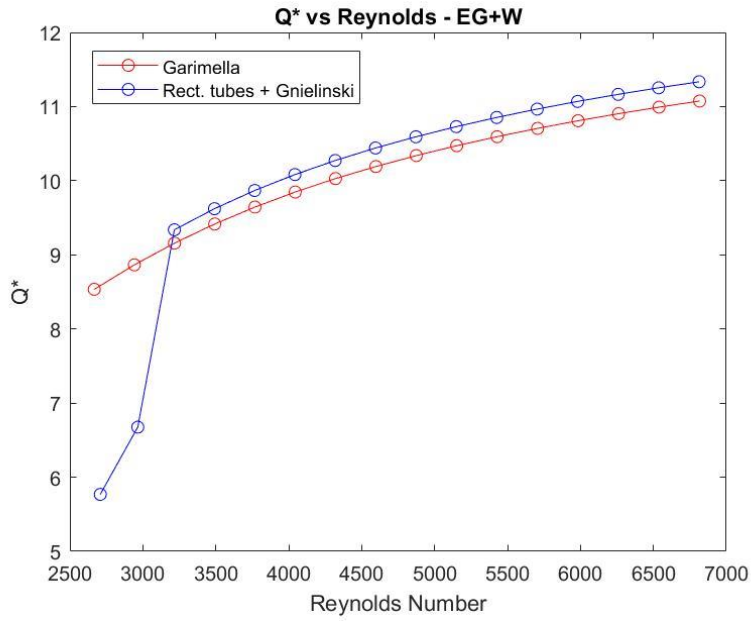

Figure 23. Q vs Reynolds for the two different correlations, using EG+W

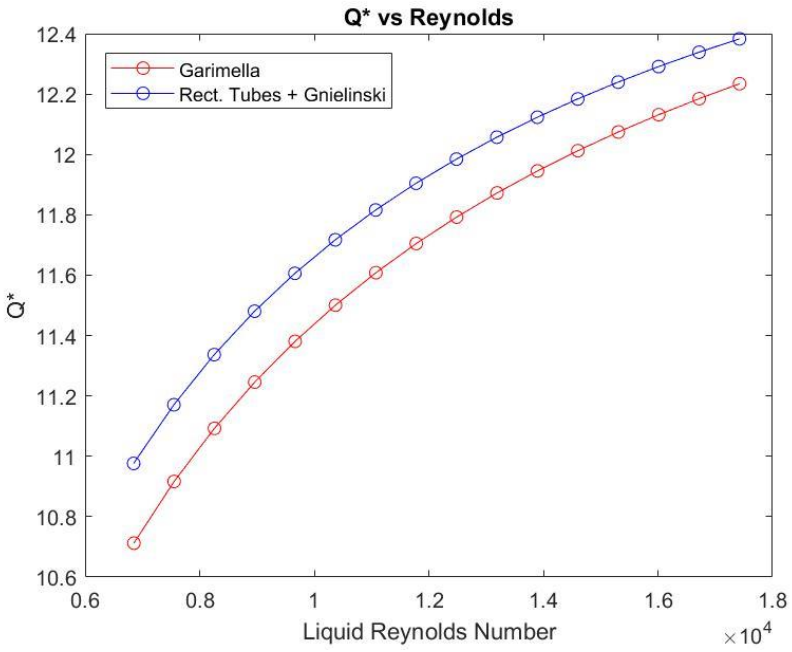

Figure 24. Q vs Reynolds for the two different correlations, using water.

On one hand, Figure 23 represents the case where the coolant is ethylene glycol + water. In this case, $Re_{Dh,liq}$ takes values under 3000, showing the discontinuity that Rectangular tubes + Gnielinski correlation presents. In contrast, the Garimella correlation, painted red, presents a continuous tendency. On the other hand, Figure 24 represents the case where the coolant used is pure water. It is interesting to see that for this case $Re_{Dh,liq}$ is always over 3000, and because of that, the Rectangular tubes + Gnielinski correlation does not present a discontinuity, as in fact, only the Gnielinski part of the correlation is used. It can be observed that Garimella and Gnielinski show a similar performance, but Gnielinski obtains always a bit higher value of heat transfer.

At this point, it has been decided to use Garimella correlation for liquid side heat transfer calculations for the next simulations.

3.3.3. Validation of air pressure drop

To validate the air pressure drop calculation, it has been compared the results obtained by the simulation with experimental results obtained in the work carried out by Carles Oliet in his doctoral thesis [42], as previously mentioned. The correlation used to calculate friction factor (13) was developed by Chang et al [30].

The experiment conditions were the same as for experiment one of section 3.3.2.1, more concretely:

- Coolant mass flow rates: [1000 Kg/h, 1500 Kg/h, 2000 Kg/h]
- Air mass flow rates: [0,14 Kg/s, 0,21 Kg/s, 0,28 Kg/s, 0,39 Kg/s]
- Inlet conditions: $T_{liq,in} = 15ºC$, $T_{air,in} = 40ºC$, $P_{liq,in} = 1{,}5\ atm$, $P_{air,in} = 1\ atm$
- Coolant: Water

The experimental data obtained is confidential, so it has been calculated the error between the simulation results and the experimental results, analogously to equation (74). The results obtained are the following ones:

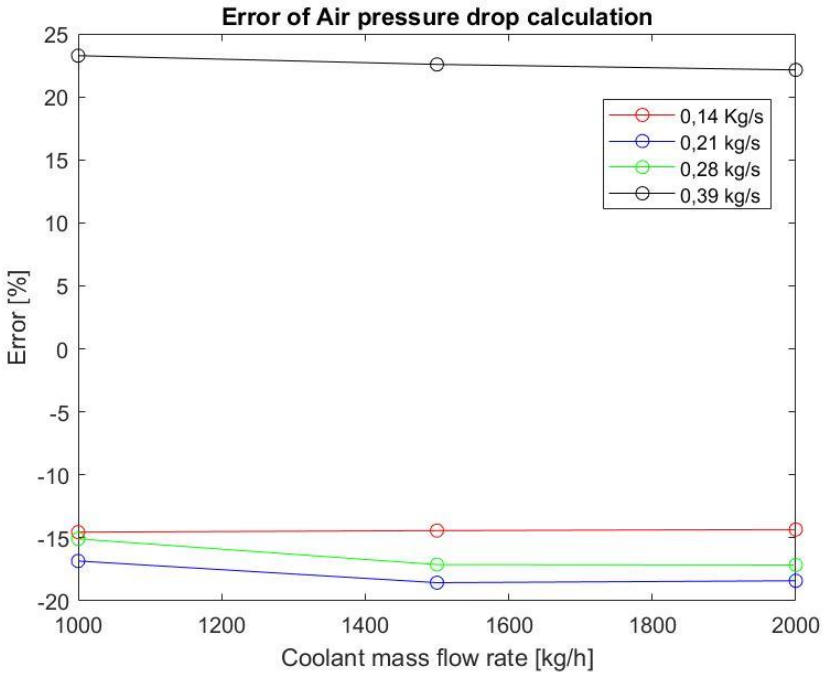

Figure 25. Air pressure drop error respect to experimental values.

Figure 25 shows that the error is between -15% and -20%, except when the mass flow rate is maximum, which the error gets to +25%. In absolute terms, the error does not reach 25%, so it has been decided to continue using this correlation for next calculations.

3.3.4. Validation of liquid pressure drop

Proceeding the same as for the validation of air pressure drop, to validate the liquid pressure drop calculation, it has been compared the simulation results with the experimental results obtained by Carles Oliet in his doctoral thesis work. The correlation used to calculate liquid friction factor is a combination of Rectangular tubes (31) + Petukhov (32) correlation.

The experiment conditions were the same as for the section before (3.3.3), more concretely:

- Coolant mass flow rates: [1000 Kg/h, 1500 Kg/h, 2000 Kg/h]
- Air mass flow rates: [0,14 Kg/s, 0,21 Kg/s, 0,28 Kg/s, 0,39 Kg/s]
- Inlet conditions: $T_{liq,in} = 15ºC$, $T_{air,in} = 40ºC$, $P_{liq,in} = 1{,}5\ atm$, $P_{air,in} = 1\ atm$
- Coolant: Water

As the experimental data obtained is confidential, it has been calculated the error between the simulation results and the experimental results, analogously to equation (74). The results obtained are the following ones:

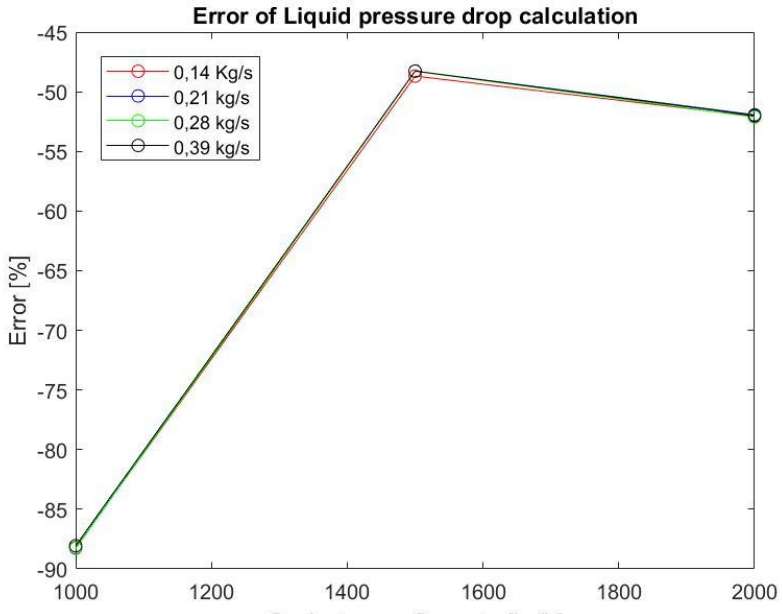

Figure 26. Liquid pressure drop error respect to experimental values.

As it can be seen in Figure 26, the correlation shows a very high error respect the experimental results. More concretely, for low coolant mass flow rates, the error is near 90%, and that's because the correlation used is Rectangular tubes, which is not very precise. Nevertheless, when the mass flow rate is higher the correlation used is Petukhov, which shows less error but still very high, near 50%.

An important point to note is that the code does not take into account the pressure losses at the inlet and outlet connections of the radiator, neither the friction in the distribution tanks, and neither the inlet and outlet effects in the rectangular tubes. Even so, the calculation has been carried out to confirm that the order of magnitude is correct, but due to the effects mentioned above, the validation cannot be closed and a more complete code would be needed. It would also be interesting to find a correlation for this application that better describes the behavior in the laminar regime and the transition zone towards turbulent regime. It is important to notate that this aspect should be improved in order to get more realistic values of pressure drop.

4. Results

4.1. Normal working conditions results

Once the code is validated, it has been obtained the results of the simulation for typical working conditions of this type of automotive radiator. As commented before, the results are presented as $X^* = \frac{X_{sim}}{X_{ref}}$, where X is a general variable. This is to not reveal confidential data that has been used for the validation of the code, and which cannot be shown.

In this section it is shown the results for the normal working conditions, in which the air gets heated and the coolant is cooled. The inlet conditions of the simulation are for this case the following ones:

- $T_{air,in} = 40ºC$
- $T_{liq,in} = 95ºC$
- $P_{air,in} = 1\ atm$
- $P_{liq,in} = 1{,}5\ atm$

In this way, it is the liquid that is refrigerated by the air that enters from the outside, while the air gets heated.

The following results have been obtained for a matrix of liquid and air mass flows.

- Coolant mass flow rates: 1000 kg/h to 2500 kg/h in intervals of 100.
- Air mass flow rates: [0,14 kg/s, 0,21 kg/s, 0,28 kg/s, 0,39 kg/s]
- Coolant used: Ethylene-glycol + water at 50% in mass.
- Number of control volumes: N=60.

It is plotted the heat transfer rate obtained, liquid outlet temperature, air outlet temperature, and the pressure drop for liquid side and air side.

4.1.1.1. Heat transfer rate

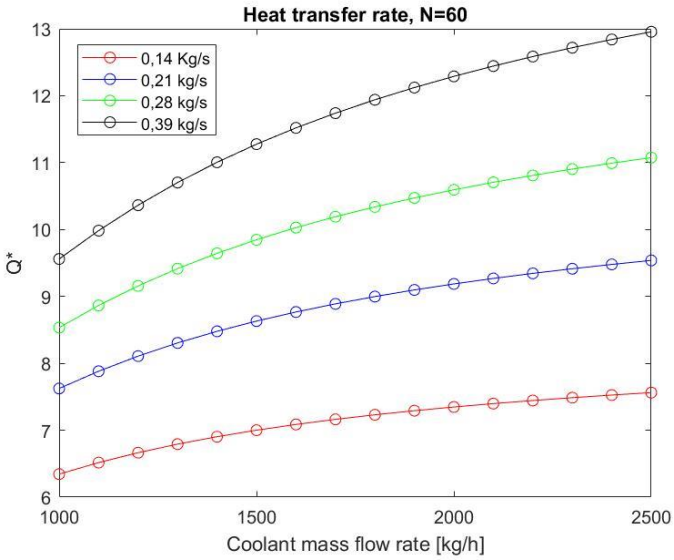

Figure 27. Heat transfer rate for different mass flow rates.

In Figure 27 it can be observed that the heat transfer rate highly depends on the air and liquid mass flow rates. As expected, it is higher when the fluid flow rates increase. It can also be seen a greater influence on the heat transfer rate of the air flow, due to the relative importance of the thermal resistances. The higher the liquid mass flow rate, the less effect its increase has on the heat transfer rate, as the thermal resistance of the liquid becomes less relevant.

4.1.1.2. Outlet liquid temperature

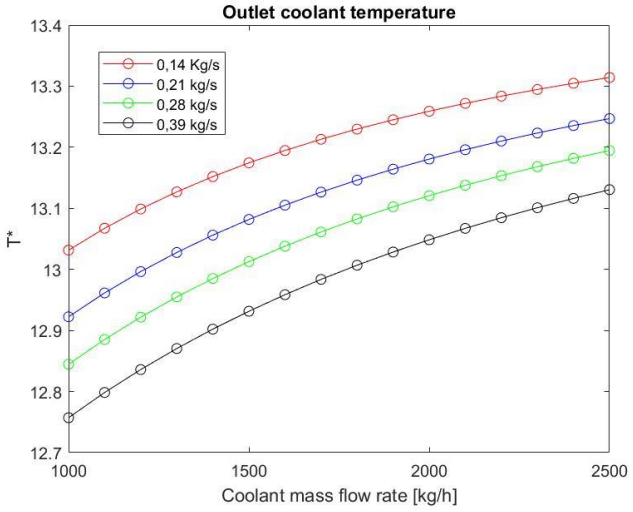

Figure 28. Outlet coolant temperature for different mass flow rates.

Figure 28 shows the outlet temperature for liquid in each case. It can be seen that when air mass flow increases, the outlet liquid temperature decreases, for a constant liquid mass flow, and when coolant mass flow increases, the outlet coolant temperature does so, for a constant air flow rate. This behavior follows the logic, regarding the inlet conditions.

4.1.1.3. Mean outlet air temperature

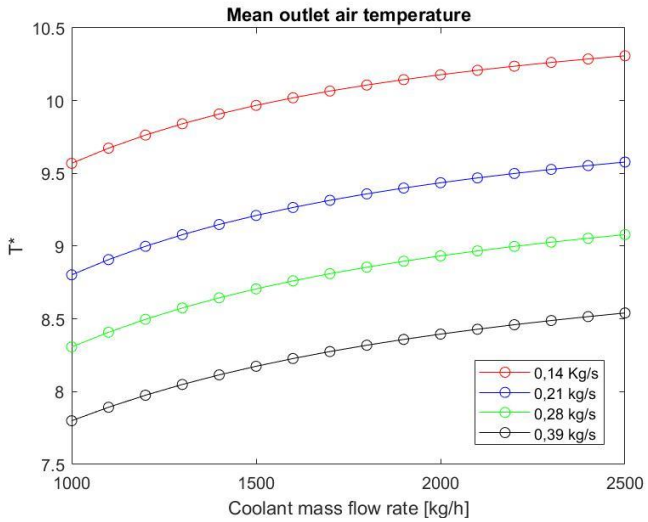

Figure 29. Mean outlet air temperature for different mass flow rates.

Figure 29 shows the mean outlet temperature for air. It is the mean value, as the outlet air temperature changes in the tube direction. It can be seen that it increases when decreasing air mass flow. Compared to liquid temperature variation, air temperature variation is much higher, as it is a gas. It can also be seen that temperature variation highly depends on both mass flow rates.

4.1.1.4. Liquid pressure drop

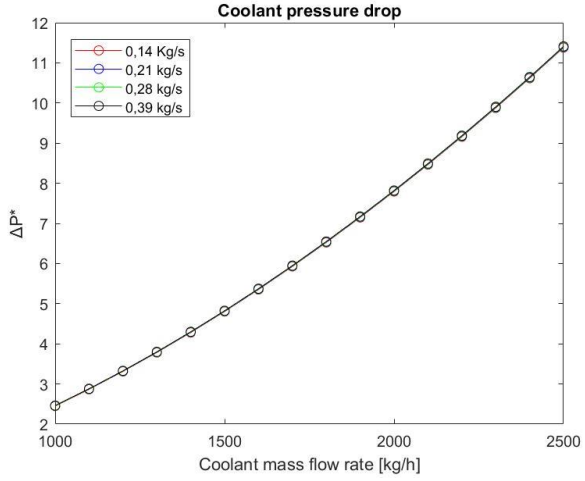

Figure 30 Liquid pressure drop for different mass flow rates.

Figure 30 shows the pressure drop calculated by means of (31) and (32). It can be seen that pressure drop at liquid side depends only on the coolant flow rate. The variation of the pressure drop increases when coolant mass flow rate does so.

4.1.1.5. Air pressure drop

The pressure drop for the air side has been calculated by means of Chang et al correlation (13). As it depends more on the air mass flow rate than on the coolant mass flow rate, it has been obtained the plot with the air mass flow rate on the horizontal axis, as it can be seen in next figure. In this case, the liquid mass flow rate has taken values of 1000 kg/h, 1500 kg/h, 2000 kg/h and 2500 kg/h, while the air mass flow rate has taken values from 0,14 kg/s to 0,38 kg/s in intervals of 0,02 Kg/s.

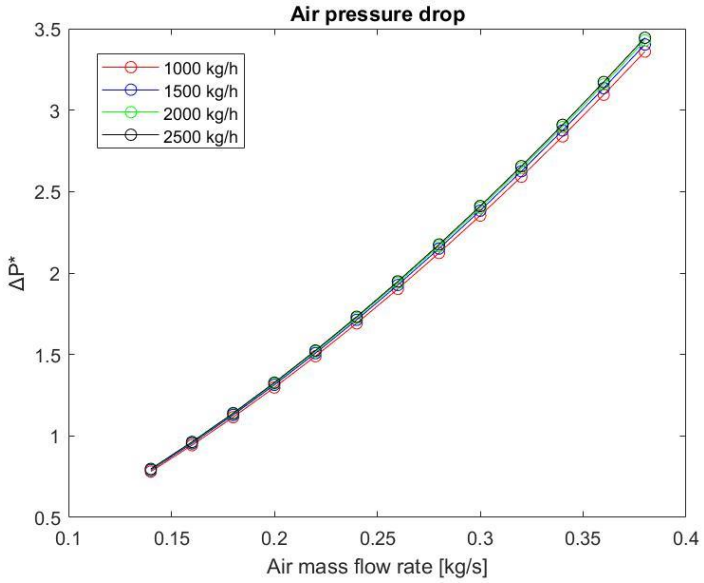

Figure 31. Air pressure drop for different mass flow rates.

Figure 31 shows that the pressure drop of the air practically does not depend on the mass flow of the liquid, as expected. For the larger air mass flow values, the pressure drop takes values that corresponds to about 0.7% of the inlet pressure. As expected, the pressure drop in the liquid side is much higher than for the air, as one is a liquid and the other a gas.

4.2. Parametric study results on louver parameters

For this section, the thermal behavior of the radiator has been analyzed by changing the angle and length of the louver fin. As the louvered fins are a typical characteristic of automotive radiators, it is wanted to see how these two louver parameters influence the heat transfer rate and the pressure drop.

Taking into account that these parameters affect basically to the are side part of the radiator, it has been considered a constant value for liquid mass flow rate. Concretely, the working conditions are the following ones:

- $T_{air,in} = 40ºC;\ T_{liq,in} = 95ºC;\ P_{air,in} = 1\ atm;\ P_{liq,in} = 1{,}5\ atm$
- Air mass flow rates: [0,14 kg/s; 0,21 kg/s; 0,28 kg/s; 0,39 kg/s].
- Liquid mass flow rate: 1000 kg/h.
- Coolant: EG + Water at 50% in mass.
- N=60

4.2.1. Louver angle influence

To see the influence that louver angle has on the thermal behavior, the louver angle θ has taken values from 8º to 30º in intervals of 1º. This range for θ has been chosen regarding the conditions analyzed in Chang et al article [29], where θ varied between these two values. In this case, Ll has a constant value of $Ll = 0{,}75 * Fl$, as in the normal conditions.

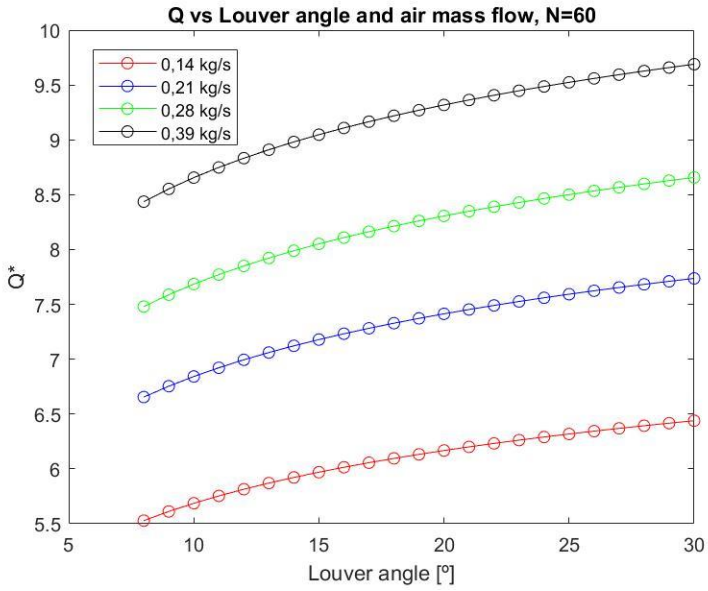

Figure 32. Heat transfer rate for different louver angles and air mass flows.

Figure 32 shows that for all the air mass flows, when θ increases, the heat transfer rate does so, but as θ becomes larger, the variation in the heat transfer rate is smaller. Nevertheless, it shows that θ has an important influence on heat transfer, as for example, comparing $\theta = 8º$ to $\theta = 30º$, the heat transfer enhancement is 21,5% approximately.

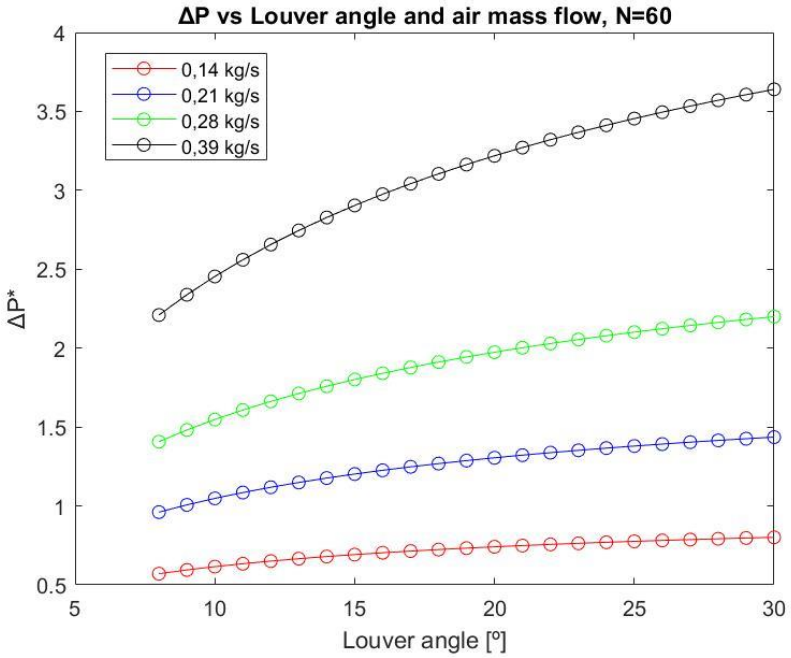

Figure 33. Air pressure drop for different louver angles and air mass flows

Referring to pressure drop, it can be observed in Figure 33 that it also increases when θ does so, but it also happens that the plots lose slope as θ increases. It can be seen that for higher air mass flow rates, the pressure drop increases more markedly. For example, comparing $\theta = 8º$ and $\theta = 15º$, the pressure drop increases 34,1% when air mass flow is 0,39 kg/s, while it increases 26,8% when air mass flow is 0,28 kg/s.

4.2.2. Louver length influence

For the louver length analysis on the thermal behavior, it has been taken run the simulation for different Ll values. For the normal simulation the Ll was considered as $Ll = 0{,}75 * Fl$, so in this case the proportion between Ll and Fl varied in the range of 0,5 to 0,9, in intervals of 0,02. This range for Ll has been chosen regarding the conditions analysed in Chang et al article [29]. For these results, θ has been kept constant at $\theta = 26º$, which was the value for the normal conditions.

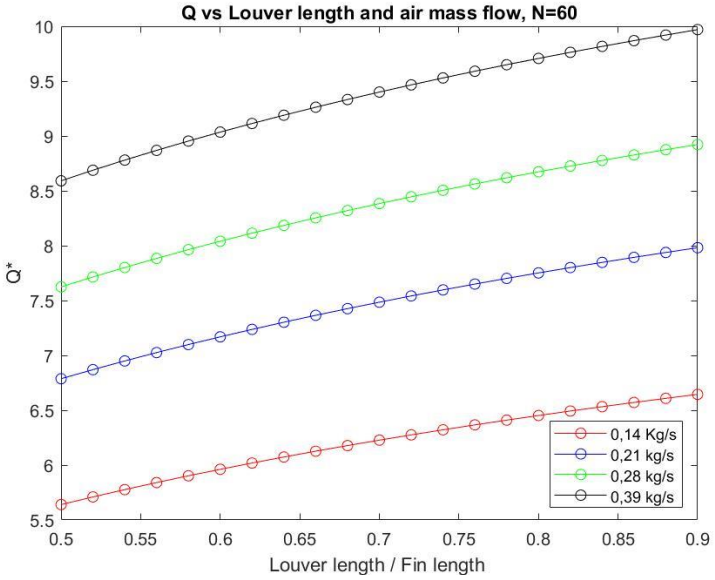

Figure 34. Heat transfer rate for different louver length and air mass flows.

Figure 34 shows how heat transfer increases when louver length does so. It also can be seen that the variation of heat transfer respect louver length, is similar for all different air mass flow rates.

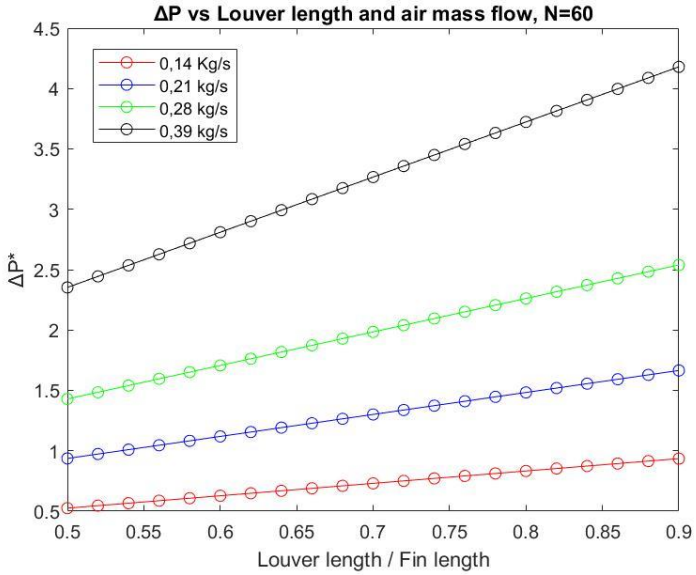

Figure 35. Air pressure drop for different louver length and air mass flows.

In Figure 35 it can be seen that when louver length increases the pressure drop does so, and it is interesting to observe that the slope of the pressure drop versus louver length plot, increases when air mass flow rate does so.

4.3. Implementation of nanofluid coolant in the simulation code

This part of the project is dedicated to the implementation to the developed simulation code presented in part 3, of any of the technologies previously mentioned in the section 0, on the State-of-the-art of automotive radiators. Regarding the different possibilities of existing trends in vehicle radiators field, it has been chosen the use of nanofluids coolants as the one to try to implement.

There is a wide range of literature on the use of nanofluids as coolants in heat exchangers in general. Even so, there's not a clear concordance on the results of the articles and investigations. Although great part of they conclude that in general the use of nanofluids as coolants enhances the heat transfer phenomena, it is not exactly determined how much enhancement is obtained, or if the improvements are just in some concrete working conditions or nanoparticles, or even if in some cases the enhancement is not considerable at all. Facing this situation of some uncertainty, it has been wanted to see how the application of nanofluids is affecting the heat transfer phenomena in this study case, in this simulation.

4.3.1. Nanofluid involved

A high number of different nanoparticles have been used for heat transfer applications in nanofluids, and the one selected for this study is Al_2O_3. There are different articles and investigations about the use of Al_2O_3 – water nanofluid. In order to implement the use of this nanofluid in the simulation, it is necessary to find expressions for the thermophysical properties of the nanofluid in question, and for the heat transfer correlations. The current literature on the subject contains various correlations of the properties, but this is a complicated task, since these expressions change depending on the working temperature range, the size of the nanoparticle, the base fluid, or the concentration of the nanoparticle. Regarding the situation, the calculation of thermophysical properties is made using the following expressions:

- For thermal conductivity, Ghanbarpour et al (2014) proposed:

$$\lambda_{nfl} = \lambda_{bfl} * [1 + 3{,}5(\varphi * 100) + 2{,}5(\varphi * 100)^2][32] \quad (75)$$

- For viscosity, Meybodi et al (2016) proposed:

$$\mu_{nfl} = \mu_{bfl} * \frac{A1+A2\exp\left(\varphi/_{d}\right)+A3\,(\exp\,(\varphi/_{d}))^2+A4\,(\exp\,(\varphi/_{d}))^3}{A5+A6\frac{\ln\,(d)}{T}+A7\frac{(\ln\,(d))^2}{T}}$$ [33]

(76)

Where:

$$A1 = 1{,}3354064976 * 10^2;$$

$$A2 = -3{,}4382413843 * 10^2;$$

$$A3 = 2{,}9011804759 * 10^2;$$

$$A4 = -7{,}8993120761 * 10^1;$$

$$A5 = 9{,}1161630781 * 10^{-1};$$

$$A6 = 3{,}2330142333 * 10^1;$$

$$A7 = -1{,}1732514460 * 10^1;$$

- For density, Pak and Cho (1998) proposed:

$$\rho_{nfl=}\varphi * \rho_{npart} + (1-\varphi) * \rho_{bfl}$$ [34]

(77)

- For specific heat, Pak and Cho (1998) proposed:

$$Cp_{nfl=}\varphi * Cp_{npart} + (1-\varphi) * Cp_{bfl}$$ [34]

(78)

- For Nusselt number, Vajjha, Das and Ray (2015) proposed:

$$Nu_{nfl} = 0{,}023 * {Re_{Dh,liq}}^{0,8} * {Pr_{liq}}^{0,3} * (1 + 0{,}1771 * \varphi^{0,1465})$$ [35]

(79)

It is important to notate that (79) is a correlation that was obtained in experiments with a nanofluid in which the nanoparticle was Al_2O_3 and with a base fluid of ethylene glycol and water, instead of pure water. Nevertheless, it has been assumed that the phenomenology of the problem does not depend on these two different base fluids, so it has been considered reasonable to use it also in the case where the base fluid is pure water.

There are properties of the nanoparticle that are needed for the simulation of this nanofluid, which are:

$$\rho_{npart} = 3900\ kg/m^3$$

$$Cp_{npart} = 880\frac{J}{kg\ K}$$

4.3.2. Simulation and results obtained

At this point, it has been simulated the nanofluid behavior in the radiator used in this project. Regarding the imposition of conditions by the use of heat transfer and properties correlations of this nanofluid, it has been decided to run the simulation for a constant nanofluid concentration, and for a certain nanoparticle size. The simulation has been run for different mass flow rates of air and coolant. The conditions are the following ones:

- $P_{air,in} = 100000\ Pa;\ T_{air,in} = 40ºC; P_{liq,in} = 150000\ Pa;\ T_{liq,in} = 15ºC;$
- $\varphi = 0.03$
- $d = 25\ nm$
- $\dot{m}_{air} = [0{,}14; 0{,}21; 0{,}28; 0{,}39]\ kg/s$
- $\dot{m}_{liq}$ between $1000\ kg/h$ and $2500\ kg/h$ in intervals of $150\ kg/h$
- Coolant: Al_2O_3 nanofluid, with water as base fluid.

To see if there is heat transfer enhancement, it has also been calculated the heat transfer for the same conditions in two more situations. One situation is using the Garimella correlation for Nusselt number instead of (79), and the other situation is using pure water as coolant. The results are the following ones:

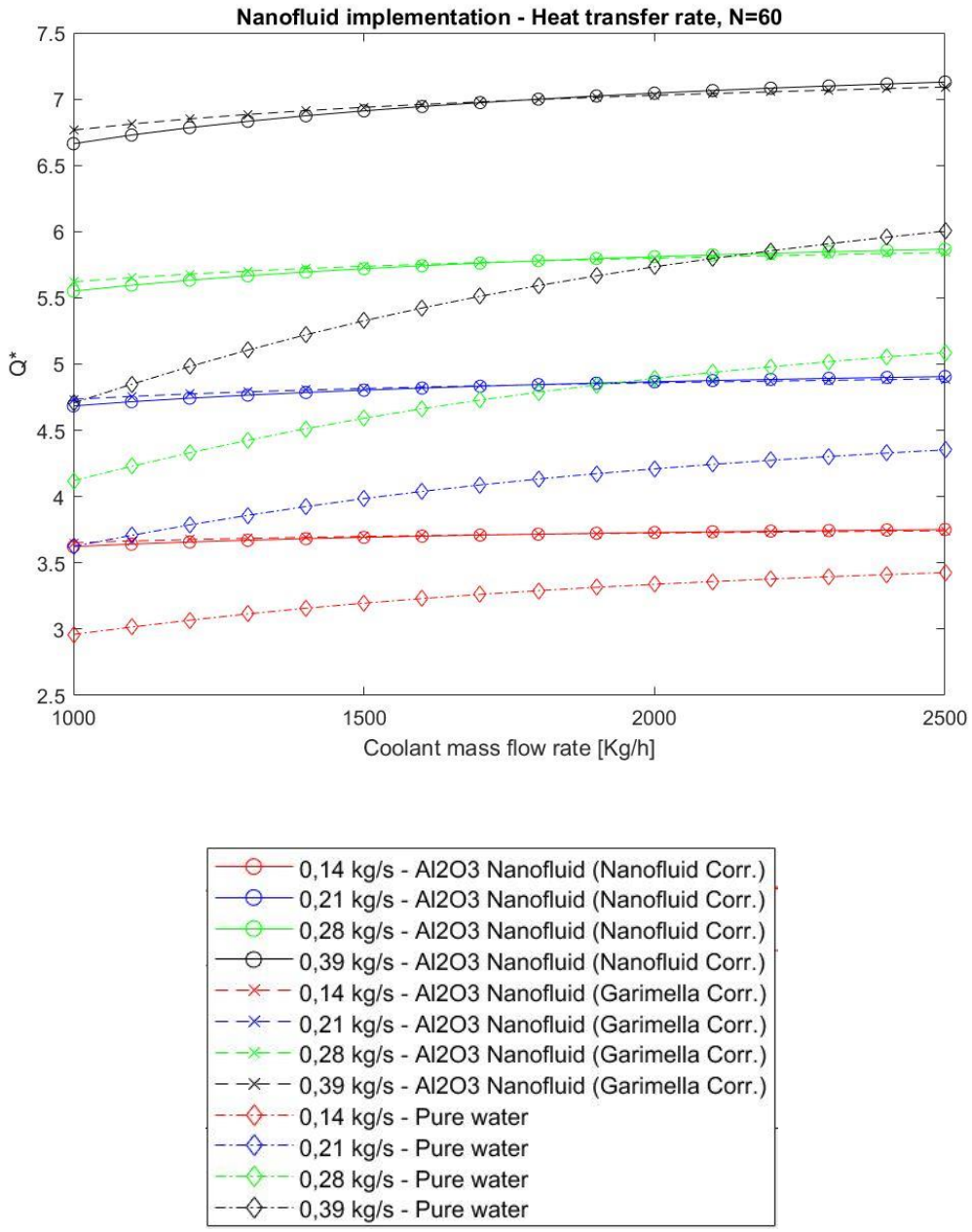

Figure 36. Heat transfer rate for different mass flows and for the 3 different situations.

In Figure 36 it is represented the heat transfer for all the combinations of mass flow rates, and also comparing the cases of nanofluid correlation, Garimella correlation, and the pure water case. It can be seen that there's a clear heat transfer rate enhancement with the addition of nanofluid, as when the coolant is pure water the heat transfer is lower for all the cases. It can also be observed that there's not too much difference in heat transfer rate between the use of nanofluid correlation and the Garimella correlation. It can be seen that when nanofluid is used and coolant mass flow increases, the heat transfer rate also increases but only slightly. It is worth noting that the heat transfer enhancement is greater when air mass flow rate increases, and for low liquid mass flow rates.

To illustrate this enhancement, Table 1 is presented:

Air mass flow rate	0,39 [kg/s]	43,77%	30,26%	22,55%	18,10%
	0,28 [kg/s]	36,45%	25,02%	18,53%	14,84%
	0,21 [kg/s]	29,90%	20,88%	16,24%	12,33%
	0,14 [kg/s]	22,44%	15,77%	11,55%	9,21%
		1000,00 [kg/h]	1500,00 [kg/h]	2000,00 [kg/h]	2500,00 [kg/h]
		Liquid mass flow rate			

Table 1. Percentage of heat transfer enhancement when using nanofluid, for different mass flow rates.

Nevertheless, for this nanofluid implementation, it has to be pointed that Garimella correlation is not designed for nanofluid applications, so in this case, applying the Garimella correlation for a nanofluid application is like just changing the thermophysical properties of the coolant, but not the heat transfer correlation.

5. Economic study

For the economic study of this project, it has been taken into account the following aspects. It has to be considered that the project has not required to go to the university, which has avoided travel costs. It is also important to remark that, as it is a simulation study, there have been not costs related with experimental procedures.

- Computer cost and consumption

Assuming the cost of the computer as 1200€, and the used time/computer lifetime as 0,08, the computer cost is 96€. Moreover, it has been considered the cost due to the energy consume, which is 0,02 kW for the computer, during 500 hours work, and considering a mean price of kWh in Spain of 0,39 €/kWh [36], the cost of energy consumption is 3,9€. The total computer cost and consumption cost is 99,9€.

- MATLAB license

This project has been developed using MATLAB software, for which an annual license costs 840€.

- Time dedicated by the student

The dedicated time by the student has been estimated as 700 hours, and the price per hour has been considered 20 €/h. In total, the cost due to the time dedicated is 14000€.

The costs are presented in the following table.

Concept	*Usage time / lifetime*	*Price (€)*	*Hours*	*Consumed power (kW)*	*Price of kWh (€/kWh)*	*Price/Hour (€/h)*	***Cost (€)***
Computer	0,08	1200	500	0,02	0,39	-	**99,9**
Anual Matlab License	-	840	-	-	-	-	**840**
Time dedicated	-	-	700	-	-	20	**14000**
						TOTAL COST	**14940**

Table 2. Itemised total cost

As it can be seen, the total budget needed for this project is 14940 €.

6. Environmental study

Any work or activity that is carried out has an impact on the environment that must be quantified. This section assesses the environmental impact associated with carrying out this project. It should be noted that this is not, in general terms, a project that involves large amounts of energy consumption or many actions of considerable environmental impact, unlike other projects that may be more significant in this aspect.

To quantify the environmental impact, it has been used as measure unit the equivalent Kg of CO_2 emitted. For this project, it has been considered the environmental impact of the energy consumed by the computer and for the computer manufacturing. Thus, the impact is calculated as:

- Electricity consumed: $500\ h * 0{,}02\ kW * \frac{0{,}259\ kg\ CO2}{kWh} = 2{,}59\ kg\ CO_2$
- Computer manufacturing: $0{,}08\ \frac{Usage\ time}{life\ time} * 248{,}5\ \frac{Kg\ CO2}{one\ laptop} = 19{,}88\ kg\ CO_2$

Taking into account that, the mix of electric net in Spain is 0,259 Kg CO_2 / kWh, in April 2022 [37], and the kg of CO_2 emitted due to the manufacturing of one laptop is assumed as 248,5 Kg CO_2 [38].

Therefore, the total environmental impact of the project is estimated at 22,47 Kg CO_2.

However, in terms of environmental impact, it should also be considered, although it is difficult to quantify, that this project can contribute to the optimization of automotive radiators, and consequently help to achieve lower fuel consumption by vehicles, and thus reduce CO_2 emissions into the atmosphere.

Conclusions

Regarding the objectives initially raised, it can be concluded that the thermal behavior of a typical vehicle radiator has been understood. The development of a code that allows the simulation of a typical vehicle radiator has been achieved, although some aspects of the code could be improved or reconsidered in order to obtain more precise results. It also has been possible to apply the multi ε-NTU methodology and to acquire the needed knowledge to use it in a properly way.

Regarding the results obtained for the run simulations, it could be seen in the section of validation of calculations, that the results obtained with respect to the experimental results had an error of between 5% and 20% in heat transfer rate, and similar for the air pressure drop. These results have been considered as good, but it would be interesting to find a way to reduce this error, either by proposing other correlations, or another way of calculating the geometries, or another way of analyzing the radiator as a whole and not just one tube, or using a different methodology than ε-NTU. Liquid pressure drop calculation showed even higher error, so the correlation used to calculate it should be reconsidered in order to get more precise results. Nevertheless, it has to be noted that results showed coherent values in heat transfer and outlet temperatures, and air pressure drops, which indicated that the code worked properly. It also has been seen that different working conditions can be simulated, as in some cases the air transferred heat to the liquid, and in some other cases, it was the liquid transferring heat to the air.

It also can be concluded that the implementation of nanofluids in the simulation has made a considerable enhancement in the heat transfer rate. However, it has to be pointed the difficulty to find properties, heat transfer and friction factor correlations for certain nanofluids, as the correlations varied depending on the nanofluid concentration, the nanoparticle and its size, the base fluid used and the working temperature range, among other parameters. For this reason, it was hard to find a concrete case in which was possible to run the simulation.

As far as the State-of-the-art of the topic is concerned, the main evolutions and trends in the world of automotive radiators have been identified. It is worth highlighting the great future potential of polymeric radiators, given their lower production costs. The use of surface coatings or nanofluids as coolants have also been implemented in several studies, and in general have had a positive impact on thermal behavior. Still, there is considerable discrepancy regarding the improvement that nanofluids can bring, due to a great diversity of conditions in the present studies. In general, for these new automotive radiator technologies, it is commented that the lack of further experimental results makes it difficult to quantify more precisely the improvement they bring.

Forthcoming work

Arrived so far, there is some forthcoming work that could be done in this project. It would be interesting to take the code one level further in terms of programming, in order to be able to make a more comfortable use of it. It would also be required to find more accurate heat transfer and friction factor correlations, to try to reduce the error respect experimental results. Another task, could be to obtain experimental results in order to have more data to compare with the simulation results.

On the other hand, regarding the implementation of improvements in automotive radiators, it would be attractive to try to implement heat transfer improvement using new coatings, as explained in the section 2.3.2. Concerning the implementation of the use of nanofluids, further research would also have to be done in order to obtain various correlations of thermal properties, heat transfer and friction coefficient, so that simulations with different ranges of nanofluid concentration, nanoparticle size, different base fluids or different nanoparticles could be performed, so that more extensive and generic results could be obtained.

Acknowledgements

The author would like to thank Carles Oliet, director of the project, for proposing the topic and for guiding and helping whenever it was necessary throughout the development of the project.

Also, thanks to family and friends, who have shown support and understanding throughout the duration of the project.

Bibliography

Bibliographical references

[1] Samiolo, M. and Verdin, P., 2022. Numerical modelling of a finless heat exchanger layout for electric vehicle application. *Applied Thermal Engineering*, 211, p.118506.

[2] IEA. 2022. *Global EV Outlook 2022 - Data product - IEA*. [online] Available at: <https://www.iea.org/data-and-statistics/data-product/global-ev-outlook-2022>.

[3] NanoSlic Coatings. 2022. *What are Nanocoatings? - NanoSlic*. [online] Available at: <https://nanoslic.com/about-nanocoatings/>.

[4] Pungaiah, S. and Kailasanathan, C., 2020. Thermal Analysis and Optimization of Nano Coated Radiator Tubes Using Computational Fluid Dynamics and Taguchi Method. *Coatings*, 10(9), p.804.

[5] Pungaiya, S. and Kailasanathan, C., 2018. A Review of Surface Coating Technology to Increase the Heat Transfer. *International Journal of Mechanical Engineering and Robotics Research*, pp.458-465.

[6] Sujith Kumar, C., Suresh, S. and Rajiv, K., 2012. Heat Transfer Enhancement by Nano Structured Carbon Nanotube Coating. *International Journal of Scientific & Engineering Research*, 3(6).

[7] Rajput, K. and Kulkarni, A., 2014. A Review on Effect of Perforation and Carbon Nanotubes Coating on Heat Transfer Augmentation. *International Journal of Innovative Research in Science, Engineering and Technology*, 3(2).

[8] Jadar, R., Shashishekar, K. and Manohara, S., 2017. Nanotechnology Integrated Automobile Radiator. *Materials Today: Proceedings*, 4(11), pp.12080-12084.

[9] New Atlas. 2022. *Nanostructure coatings remove heat four times faster*. [online] Available at: <https://newatlas.com/nanostructure-coatings-remove-heat-four-times-faster/15384/>.

[10] Park, Y. and Jacobi, A., 2008. Polymer-Tube-Bundle Heat Exchanger for Liquidto- Gas Applications. *International Refrigeration and Air Conditioning Conference*,.

[11] Krásný, I., Astrouski, I. and Raudenský, M., 2016. Polymeric hollow fiber heat exchanger as an automotive radiator. *Applied Thermal Engineering*, 108, pp.798-803.

[12] T'Joen, C., Park, Y., Wang, Q., Sommers, A., Han, X. and Jacobi, A., 2009. A review on polymer heat exchangers for HVAC&R applications. *International Journal of Refrigeration*, 32(5), pp.763-779.

[13] Zaheed, L. and Jachuck, R., 2004. Review of polymer compact heat exchangers, with special emphasis on a polymer film unit. *Applied Thermal Engineering*, 24(16), pp.2323-2358.

[14] Raudensky, M., Brozova, T. and Astrouski, I., 2016. Polymeric hollow fiber heat exchangers. *14th International Conference on Simulation and Experiments in Heat Transfer and its Applications*.

[15] Kroulíková, T., Kůdelová, T., Bartuli, E., Vančura, J. and Astrouski, I., 2021. Comparison of a Novel Polymeric Hollow Fiber Heat Exchanger and a Commercially Available Metal Automotive Radiator. *Polymers*, 13(7), p.1175.

[16] Hajatzadeh Pordanjani, A., Aghakhani, S., Afrand, M., Mahmoudi, B., Mahian, O. and Wongwises, S., 2019. An updated review on application of nanofluids in heat exchangers for saving energy. *Energy Conversion and Management*, 198, p.111886.

[17] Delavari, V. and Hashemabadi, S., 2014. CFD simulation of heat transfer enhancement of Al 2 O 3 /water and Al 2 O 3 /ethylene glycol nanofluids in a car radiator. *Applied Thermal Engineering*, 73(1), pp.380-390.

[18] Tijani, A. and Sudirman, A., 2018. Thermos-physical properties and heat transfer characteristics of water/anti-freezing and Al2O3/CuO based nanofluid as a coolant for car radiator. *International Journal of Heat and Mass Transfer*, 118, pp.48-57.

[19] Vajjha, R., Das, D. and Namburu, P., 2010. Numerical study of fluid dynamic and heat transfer performance of Al2O3 and CuO nanofluids in the flat tubes of a radiator. *International Journal of Heat and Fluid Flow*, 31(4), pp.613-621.

[20] Epandi, A., Salami Tijani, A., Abdulrahman, S., Kubenthiran, J. and Muritala, I., 2022. Numerical Simulation of Thermophysical Properties and Heat Transfer Characteristics of Al2O3/CuO Nanofluid with Water/ Ethylene Glycol as Coolant in a Flat Tube of Car Radiator. *Pertanika Journal of Science and Technology*, 30(2), pp.853-873.

[21] Hussein, A., Bakar, R., Kadirgama, K. and Sharma, K., 2014. Heat transfer augmentation of a car radiator using nanofluids. *Heat and Mass Transfer*, 50(11), pp.1553-1561.

[22] Hussein, A., Bakar, R., Kadirgama, K. and Sharma, K., 2014. Heat transfer

enhancement using nanofluids in an automotive cooling system. *International Communications in Heat and Mass Transfer*, 53, pp.195-202.

[23] Ruey Ong, H., Mohd Eqhwan Iskandar, W., Yapp Joo, M., Rahman Khan, M. and Khairul Anuar Mohamed, M., 2022. Effects of natural-based SiO2 nanocoolant on car radiator: Thermal profile. *Materials Today: Proceedings*,.

[24] Ramadhan, A., Azmi, W., Mamat, R., Diniardi, E. and Hendrawati, T., 2021. Experimental Investigation of Cooling Performance in Automotive Radiator using Al2O3-TiO2-SiO2 Nanofluids. *Automotive Experiences*, 5(1), pp.28-39.

[25] Prasanna Shankara, R., Banapurmath, N., D'Souza, A., Sajjan, A., Ayachit, N., Yunus Khan, T., Badruddin, I. and Kamangar, S., 2022. An insight into the performance of radiator system using ethylene glycol-water based graphene oxide nanofluids. *Alexandria Engineering Journal*, 61(7), pp.5155-5167.

[26] Tafakhori, M., Kalantari, D., Biparva, P. and Peyghambarzadeh, S., 2021. Assessment of Fe3O4–water nanofluid for enhancing laminar convective heat transfer in a car radiator. *Journal of Thermal Analysis and Calorimetry*, 146(2), pp.841-853.

[27] Hajatzadeh Pordanjani, A., Aghakhani, S., Afrand, M., Mahmoudi, B., Mahian, O. and Wongwises, S., 2019. An updated review on application of nanofluids in heat exchangers for saving energy. *Energy Conversion and Management*, 198, p.111886.

[28] Zhao, N., Li, S. and Yang, J., 2016. A review on nanofluids: Data-driven modeling of thermalphysical properties and the application in automotive radiator. *Renewable and Sustainable Energy Reviews*, 66, pp.596-616.

[29] Chang, Y., Hsu, K., Lin, Y. and Wang, C., 2000. A generalized friction correlation for louver fin geometry. *International Journal of Heat and Mass Transfer*, 43(12), pp.2237-2243.

[30] Chang, Y. and Wang, C., 1996. A generalized heat transfer correlation for louver fin geometry. *International Journal of Heat and Mass Transfer*, 40(3), pp.533-544.

[31] Garimella, S., Dowling, W., Van Der Veen, M. and Killion, J., 2001. The Effect of Simultaneously Developing Flow on Heat Transfer in Rectangular Tubes. *Heat Transfer Engineering*, 22(6), pp.12-25.

[32] Ghanbarpour, M., Bitaraf Haghigi, E. and Khodabandeh, R., 2014. Thermal properties and rheological behavior of water based Al2O3 nanofluid as a heat transfer fluid. *Experimental Thermal and Fluid Science*, 53, pp.227-235.

[33] Meybodi, M., Daryasafar, A., Koochi, M., Moghadasi, J., Meybodi, R. and Ghahfarokhi, A., 2016. A novel correlation approach for viscosity prediction of water based nanofluids of Al 2 O 3 , TiO 2 , SiO 2 and CuO. *Journal of the Taiwan Institute of Chemical Engineers*, 58, pp.19-27.

[34] Pak, B. and Cho, Y., 1998. HYDRODYNAMIC AND HEAT TRANSFER STUDY OF DISPERSED FLUIDS WITH SUBMICRON METALLIC OXIDE PARTICLES. *Experimental Heat Transfer*, 11(2), pp.151-170.

[35] Vajjha, R., Das, D. and Ray, D., 2015. Development of new correlations for the Nusselt number and the friction factor under turbulent flow of nanofluids in flat tubes. *International Journal of Heat and Mass Transfer*, 80, pp.353-367.

[36] tarifaluzhora.es. 2022. *¿Cuánto cuesta el kilovatio hora de luz (kWh) en España?*. [online] Available at: <https://tarifaluzhora.es/info/precio-kwh>.

[37] Cambio climático. 2022. *Factor de emisión de la energía eléctrica: el mix eléctrico*. [online] Available at: <https://canviclimatic.gencat.cat/es/actua/factors_demissio_associats_a_lenergia/>.

[38] Phys.org. 2022. *Factory is where our computers eat up most energy*. [online] Available at: <https://phys.org/news/2011-04-factory-energy.html>.

[39] Bell, I., Wronski, J., Quoilin, S. and Lemort, V., 2014. Pure and Pseudo-pure Fluid Thermophysical Property Evaluation and the Open-Source Thermophysical Property Library CoolProp. *Industrial & Engineering Chemistry Research*, 53(6), pp.2498-2508.

[40] n.d. *Formulae for the resolution of fluid dynamics and heat and mass transfer problems*. 3rd ed. Heat and Mass Transfer Technological Center (CTTC). Universitat Politècnica de Catalunya-BarcelonaTech (UPC), pp.1-28.

[41] Oliet, C., Oliva, A., Castro, J. and Pérez-Segarra, C., 2007. Parametric studies on automotive radiators. *Applied Thermal Engineering*, 27(11-12), pp.2033-2043.

[42] Oliet, C., 2006. *Numerical Simulation and Experimental Validation of Fin-and-Tube Heat Exchangers*. PHD Thesis. Universitat Politècnica de Catalunya.